

***MIT Joint Program on the
Science and Policy of Global Change***



**Sensitivities of Deep-Ocean Heat Uptake
and Heat Content to Surface Fluxes and
Subgrid-Scale Parameters in an Ocean GCM
with Idealized Geometry**

Boyin Huang, Peter H. Stone and Christopher Hill

Report No. 87
September 2002

The MIT Joint Program on the Science and Policy of Global Change is an organization for research, independent policy analysis, and public education in global environmental change. It seeks to provide leadership in understanding scientific, economic, and ecological aspects of this difficult issue, and combining them into policy assessments that serve the needs of ongoing national and international discussions. To this end, the Program brings together an interdisciplinary group from two established research centers at MIT: the Center for Global Change Science (CGCS) and the Center for Energy and Environmental Policy Research (CEEPR). These two centers bridge many key areas of the needed intellectual work, and additional essential areas are covered by other MIT departments, by collaboration with the Ecosystems Center of the Marine Biology Laboratory (MBL) at Woods Hole, and by short- and long-term visitors to the Program. The Program involves sponsorship and active participation by industry, government, and non-profit organizations.

To inform processes of policy development and implementation, climate change research needs to focus on improving the prediction of those variables that are most relevant to economic, social, and environmental effects. In turn, the greenhouse gas and atmospheric aerosol assumptions underlying climate analysis need to be related to the economic, technological, and political forces that drive emissions, and to the results of international agreements and mitigation. Further, assessments of possible societal and ecosystem impacts, and analysis of mitigation strategies, need to be based on realistic evaluation of the uncertainties of climate science.

This report is one of a series intended to communicate research results and improve public understanding of climate issues, thereby contributing to informed debate about the climate issue, the uncertainties, and the economic and social implications of policy alternatives. Titles in the Report Series to date are listed on the inside back cover.

Henry D. Jacoby and Ronald G. Prinn,
Program Co-Directors

For more information, please contact the Joint Program Office

Postal Address: Joint Program on the Science and Policy of Global Change
77 Massachusetts Avenue
MIT E40-271
Cambridge MA 02139-4307 (USA)

Location: One Amherst Street, Cambridge
Building E40, Room 271
Massachusetts Institute of Technology

Access: Phone: (617) 253-7492
Fax: (617) 253-9845
E-mail: globalchange@mit.edu
Web site: <http://MIT.EDU/globalchange/>

**Sensitivities of Deep-Ocean Heat Uptake and Heat Content to
Surface Fluxes and Subgrid-Scale Parameters
in an OGCM With Idealized Geometry**

Boyin Huang^{*}, Peter H. Stone, and Christopher Hill

Joint Program on the Science and Policy of Global Change, MIT

(Submitted to *J. Geophys. Res.*, November 2001

Revised in February 2002)

^{*} Corresponding author address: Boyin Huang, 77 Mass. Ave., MIT Room 54-1721,
Cambridge, MA 02139. Email: bhuang@wind.mit.edu

Abstract

Sensitivities of the net heat flux into the deep-ocean (Q_{net}) and of the deep-ocean heat content (DOC) below 700 m are studied using an ocean general circulation model and its adjoint. Both are found to have very similar sensitivities. The sensitivity to the surface freshwater flux (E-P-R) is positive in the Atlantic, but negative in the Pacific and Southern Ocean. A positive sensitivity to the downward net surface heat flux is found only in the North Atlantic north of 40°N and the Southern Ocean. The diapycnal diffusivity of temperature affects Q_{net} and DOC positively in a large area of the tropics and subtropics in both the Pacific and Atlantic Ocean. The isopycnal diffusivity contributes to Q_{net} and DOC mainly in the Southern Ocean.

Detailed analysis indicates that the surface freshwater flux affects Q_{net} and DOC by changing vertical velocity, temperature stratification, and overturning circulation. The downward net surface heat flux appears to increase Q_{net} and DOC by strengthening vertical advection and isopycnal mixing. The contribution of isopycnal diffusivity to Q_{net} and DOC is largely associated with the vertical heat flux due to isopycnal mixing. Similarly, the diapycnal diffusivity of temperature modulates Q_{net} and DOC through the downward heat flux due to diapycnal diffusion.

The uncertainties of Q_{net} and DOC are estimated based on the sensitivities and error bars of observed surface forcing and oceanic diffusivities. For DOC, they are about 0.7°K (1°K = 3.7×10^{24} J) for the isopycnal diffusivity, 0.4°K for the diapycnal diffusivity of temperature, 0.3°K for the surface freshwater flux, and 0.1°K for the net surface heat flux and zonal wind stress. Our results suggest that the heat uptake by ocean GCMs in climate experiments is sensitive to the isopycnal diffusivity as well to the diapycnal thermal diffusivity.

1. Introduction

The oceans are one of the major components of the earth climate system owing in part to its large heat capacity. The change of the earth's climate is largely regulated by how rapidly the oceans take up heat [Levitus et al., 2000 and 2001; Barnett et al., 2001]. However, this regulation by the oceans varies greatly between models and is not well constrained by observation [Forest et al., 2002]. Therefore, a better understanding of what factors affect ocean heat uptake in ocean models is a necessary step to improve the simulation of present-day climate and the projection of future climate.

Uncertainty in ocean model simulations can arise from many different sources, such as the parameterization of mesoscale eddies, surface boundary conditions, and oceanic model subgrid-scale parameters. The wind stress and freshwater flux from the atmosphere may have a large error bar due to observational limitations over the oceans [Isemer and Hasse, 1991; Schmitt et al., 1989]. The wind stress from Hellerman and Rosenstein [1983] is stronger than that from the Comprehensive Ocean Atmosphere Data Sets [da Silva et al., 1994]. The wind stress from European Centre for Medium-range Weather Forecasts (ECMWF) [Trenberth et al., 1989] seems to be very strong over the Southern Ocean. The diffusivities based on direct ocean observations may vary about ten times in different regions [Zhang et al., 2001; Ledwell et al., 2000; Jenkins, 1991; Nakamura and Cao, 2000].

Uncertainties like these can cause different model simulations to have quantitatively different results in their simulations of climate change. Many simulations show that ocean circulation and temperature are strongly affected by vertical diffusivity [Bryan, 1986; Tsujino et al., 2000; Kamenkovich and Goodman, 2000; Cummins et al., 1990; Marotzke, 1997; Scott and Marotzke, 2001]. The simulation of Hu [1996] indicated that the thermocline depth and meridional heat transport are sensitive to the vertical diffusivity. The study of Goose et al. [1999] showed that the vertical diffusion can affect the ocean ventilation, water mass properties, sea-ice distribution, and chlorofluorocarbon

uptake. The strength and stability of deep ocean circulation are critically associated with the surface freshwater and heat flux as indicated in many studies [Mikolajewicz and Voss, 2000; Zhang et al., 1999; Rahmstorf, 1996; Pierce et al., 1995; Rahmstorf, 1995; Huang and Chou, 1994; Zaucker et al., 1994; Weaver et al., 1993]. The tracer uptake of the oceans is relatively worse using constant horizontal mixing compared to isopycnal mixing [Sun, 2000; Duffy et al., 1997]. Also, the choice of surface boundary condition may have an important impact on the simulation of ocean circulation [Bugnion, 2001; Huang, 1993].

Key questions are: How do ocean diffusivities and surface forcing affect the uncertainty of the ocean heat uptake? This has not been discussed extensively in the studies cited above. What are the mechanisms relating the ocean heat uptake with diffusivities and surface forcing, and what is their relative contribution to the ocean circulation and heat capacity? We will address these questions in the rest of this paper: Section 2 is a brief description of the ocean general circulation model (OGCM), its configuration, and its adjoint. The calculated sensitivity by the adjoint model is presented in section 3. We will study the physical mechanisms revealed by the adjoint sensitivity in section 4. The uncertainty of ocean heat uptake is estimated in section 5. Section 6 is the summary.

2. Model

2.1. Configuration

We use the MIT OGCM [Marshall et al., 1997a; 1997b; 1998] and its adjoint [Giering and Kaminski, 1998; Giering, 1999; Marotzke et al., 1999]. The model ocean consists of idealized basins of the Pacific (0-130°E, 70°S-60°N) and Atlantic (130°-200°E, 70°S-70°N) separated by idealized continents at 0°E and 130°E (refer to Fig. 1a). The bottom topography of the model ocean is flat with a depth of 4.5 km except for the Drake Passage where a sill of 1.6 km is added. Because of the geometry, the resolution of the western boundary layer can be substantially enhanced by increasing just the

longitudinal resolution near the north-south boundary, without largely impacting the integration time [Kamenkovich et al., 2002]. This makes the strength of the boundary currents and the associated mixing of heat and tracers into the deep oceans much more realistic than in conventional coarse resolution GCMs. The longitudinal resolution is 1° near the eastern and western boundaries but 4° in the interior oceans. The model ocean is divided into 15 vertical levels, and the layer thickness ranges from 50 m at the surface to 550 m at the bottom.

The vertical eddy heat fluxes in the model are parameterized by diapycnal diffusive heat flux, isopycnal diffusive heat flux, and convective heat flux. The diapycnal diffusive heat flux is explicitly diagnosed, although it is implicitly calculated in the model prognostic equation. The isopycnal diffusive heat flux is based on Gent-McWilliams mixing (GM mixing, hereafter) [Gent and McWilliams, 1990; Gent et al., 1995; Redi, 1982; Gerdes et al., 1991; Griffies, 1998; Griffies et al., 1998; Danabasoglu and McWilliams, 1995; Large et al., 1997]. The convective heat flux is calculated according to convective adjustment, assuming that the ocean temperature and salinity in the adjacent layers are fully mixed when the upper layer is denser than the lower layer. The diapycnal diffusivities are set to $5 \times 10^{-5} \text{ m}^2 \text{ s}^{-1}$ for both temperature and salinity, and the isopycnal diffusivity of temperature and salinity is $1 \times 10^3 \text{ m}^2 \text{ s}^{-1}$. The maximum slope of the isopycnal surface is set to 10^{-2} . Horizontal and vertical viscosities are 5×10^4 and $1 \times 10^{-2} \text{ m}^2 \text{ s}^{-1}$, respectively.

The model ocean is driven by zonal sea surface temperature (SST), wind stress, monthly mean net surface heat flux, and annual mean zonal freshwater flux. The SST data are based on Levitus and Boyer [1994]. The wind stress is from Trenberth et al. [1989]. The net surface heat flux is obtained from Jiang et al. [1999]. The surface heat flux is calculated by

$$F_H = \rho c_p \frac{T_0 - T}{\tau} \Delta Z_1 + Q_S, \quad (1)$$

where ρ is water density, c_p is heat capacity of water, τ is a restoring time of 30 days, ΔZ_1 is the thickness of the first model layer, T_0 is observed SST, and Q_S is observed net surface heat flux. This surface boundary condition has the advantage that it can simulate both the SST and surface heat flux accurately [Jiang et al., 1999]. The surface freshwater flux is from Jiang et al. [1999]:

$$F_S = \frac{E - P - R}{\Delta Z_1} S_0, \quad (2)$$

where E , P , and R represent evaporation, precipitation and river runoff, respectively. S_0 is the standard salinity of 35 psu. More detailed description about these data sets is provided in Jiang et al. [1999] and Kamenkovich et al. [2002]. In all cases, the original data sets have been averaged zonally for the individual idealized basins before they are applied.

2.2. Spinup

The time steps for the tracer and momentum equations are 8 hours and 30 minutes, respectively. The initial model temperature and salinity are based on Levitus and Boyer [1994] and Levitus et al. [1994]. The model ocean reaches a quasi-equilibrium state for the deep ocean temperature and salinity after 5000 years of spinup.

The model simulates the water masses reasonably as shown in the barotropic and meridional overturning stream functions (Figure 1) and zonal averaged temperature and salinity (Figure 2). The transports in subpolar, subtropical, and tropical gyres are simulated at reasonable strengths in both the Atlantic and Pacific Ocean (Figure 1a), except the Antarctic Circumpolar Current is relatively strong due to idealized topography and strong wind forcing derived from ECMWF [Trenberth et al., 1989]. The transport at the North Pacific subpolar gyre is also somewhat strong when compared with the

simulation of Jiang et al. [1999] using similar surface forcing but realistic topography and the OGCM from Geophysical Fluid Dynamics Laboratory (GFDL).

The overturning transport in the Northern Hemisphere is about 20 Sv ($1 \text{ Sv} = 10^6 \text{ m}^3 \text{ s}^{-1}$) at 50°N and 1000 m, which occurs mainly in the North Atlantic (Figure 1d), and it exhibits 12 Sv of transport across the equator into the South Atlantic. The transport within the Deacon Cell [Bryan, 1991] near 60°S is about 16 Sv, which is canceled partly by the transport due to the bolus meridional velocity. The transport of Antarctic Bottom Water (AABW) is about 8 Sv at 3.5 km, which is evenly distributed in the Pacific and Atlantic (Figures 1b-d). The transports of the subtropical cells are 20 Sv near 15°N , and 16 Sv near 15°S at depth of 100 m. These transports are somewhat weaker than those in Jiang et al. [1999] except for AABW. The North Atlantic overturning transport in our simulation is slightly weaker than the simulation (24 Sv) of Kamenkovich et al. [2002] who used the same model topography and surface forcing but with the MOM2 version of the GFDL OGCM.

The zonal averaged potential temperature and salinity of the simulation in the Pacific and Atlantic are displayed in Figure 2. The simulated temperature and salinity look reasonable, although it is difficult to compare with either observations or simulations with realistic topography.

The model simulation of the vertical heat fluxes is illustrated by horizontal global averages (Figure 3). For consistency and convenience, the direction of vertical velocity and heat fluxes is defined to be positive when downward. The net heat flux

$$Q_{net} = Q_W + Q_{CV} + Q_{DD} + Q_{GM} , \quad (3)$$

is balanced mainly between diapycnal heat flux

$$Q_{DD} = \rho c_p \iint K_t \frac{\partial T}{\partial z} dx dy , \quad (4)$$

and isopycnal heat flux

$$Q_{GM} = 2\rho c_p \iint I_{ts} \left[\frac{\partial T}{\partial y} \left(\frac{\partial z}{\partial y} \right)_\sigma + \frac{\partial T}{\partial x} \left(\frac{\partial z}{\partial x} \right)_\sigma \right] dx dy . \quad (5)$$

Here K_t is diapycnal diffusivity of temperature, and I_{ts} is isopycnal diffusivity for temperature and salinity. $(\partial z / \partial y)_\sigma$ is the slope of the isopycnal surface. The advective heat flux is defined as

$$Q_w = \rho c_p \iint W T dx dy . \quad (6)$$

Here, W is the downward vertical velocity. Q_w and convective heat flux (Q_{CV}) are relatively weaker above 1 km in the Pacific Ocean, but they contribute substantially to Q_{net} in the Atlantic Ocean. The downward advective heat flux at the surface in our model (5 Wm^{-2}) is weaker than the simulation (8 Wm^{-2}) of Gregory [2000]. The net heat flux is zero below 300 m, which indicates that the model has reached quasi-equilibrium. The net heat flux looks to be unbalanced near the surface. However, this is probably an artifact due to explicit calculation of Q_{DD} , although it is treated implicitly in the model temperature equation.

2.3. Adjoint

The adjoint model constructs relationships between a so-called cost function (F_c) at the last year of a model run and a set of parameters $P_n(x, y, z)$ at a specific spatial location of the model ocean, which is defined as the adjoint sensitivity:

$$S(x, y, z) = \frac{\partial F_c}{\partial P_n(x, y, z)}, \quad n = 1, N. \quad (7)$$

The advantage of the adjoint model is that the sensitivities of F_c to the parameter $P_n(x, y, z)$ at all grid points can be derived in a single adjoint run, while a traditional

sensitivity study can only test one single grid point for each perturbation. Further, a single adjoint model run can include many parameters ($N > 1$). Because of these advantages, adjoint models have been applied in data analysis [Winguth et al., 1998], data assimilation [Kalnay et al., 2000; Malanotte-Rizzoli, 1998], and sensitivity studies [Marotzke et al., 1999; Waelbroeck and Louis, 1995]. The disadvantage, however, is that the adjoint model can only consider a single scalar variable as a cost function, while the traditional sensitivity study can provide the 3-dimensional impact. The algorithm deriving the adjoint sensitivity in (7) is accomplished by a tangent linear and adjoint model compiler, which is documented in Giering and Kaminski [1998], Giering [1999], and Marotzke et al. [1999].

In our study of deep-ocean heat content (DOC, hereafter), we define a cost function which is proportional to the mean ocean temperature below H_d (700 m):

$$F_c = \bar{T}(z < -H_d) \propto \rho c_p \int_{-H}^{-H_d} \iint T dx dy dz. \quad (8)$$

Here, T is the annual mean potential temperature at the end of the adjoint run. This F_c can be thought of as the DOC below 700 m after multiplying by a factor of $3.7 \times 10^{24} JK^{-1}$. The selection of 700 m is to exclude the major thermocline. Considering the uncertainties in surface forcing and oceanic diffusivities in simulations of ocean temperature, we focus on the following seven parameters in our adjoint sensitivity study: the surface freshwater flux (E-P-R), downward net surface heat flux (Q_s), zonal and meridional wind stress (τ_x, τ_y), diapycnal diffusivities of temperature (K_t) and salinity (K_s), and isopycnal diffusivity for temperature and salinity (I_{ts}). The adjoint model runs for 500 years to estimate the sensitivities indicated in (7) at the time scale of 500 years. In the following section, we will present the sensitivity distribution of DOC to these seven parameters in the form of mean temperature.

3. Adjoint sensitivity

3.1. DOC sensitivity to surface forcing

The DOC sensitivity to the surface freshwater flux (E-P-R) in the Atlantic is opposite to that in the Pacific (Figure 4a). The sensitivity is about 4 to $8 \times 10^4 \text{ Ksm}^{-2}$ in the Atlantic, $-2 \times 10^4 \text{ Ksm}^{-2}$ in the Pacific, and $-8 \times 10^4 \text{ Ksm}^{-2}$ in the Southern Ocean south of 50°S . The interpretation of these sensitivities is that if evaporation increases or precipitation decreases in the Atlantic Ocean, DOC will increase as indicated in (7). The situation in the Pacific and South Ocean is opposite to that in the Atlantic. The distribution of DOC sensitivity seems to be associated directly with the thermohaline circulation which sinks in the Atlantic and upwells in the Pacific. The sign of DOC sensitivity is also consistent with the study of Rahmstorf [1996; 1995]. We will revisit this issue in section 4.1.

The sensitivity of DOC to the net surface heat flux (Q_s) is only notable in the North Atlantic north of 40°N and in the Southern Ocean (Figure 4b). The magnitude of the sensitivity is about $2 \times 10^{-5} \text{ Km}^2\text{W}^{-1}$. This means that when downward Q_s increases in the North Atlantic or Southern Ocean, DOC will increase. In addition, weaker sensitivities are exhibited in the northeast corner of the North Pacific ($5 \times 10^{-6} \text{ Km}^2\text{W}^{-1}$), and in the South Atlantic between 40°S and 55°S (1.5×10^{-5} and $-1 \times 10^{-5} \text{ Km}^2\text{W}^{-1}$). DOC is not sensitive to Q_s in the tropics and subtropics of both the Pacific and Atlantic. The absorption of surface heat by the deep ocean in high latitudes where convection is occurring agrees with Huang and Liu [2000].

The DOC sensitivity to the zonal wind stress (τ_x) is zonally distributed, and its sign alternates at different latitudinal belts (Figure 4c). The width of these belts is narrower in the South Atlantic than in the South Pacific. The magnitude of the sensitivity is higher in the South Atlantic ($2 \times 10^{-2} \text{ Km}^2\text{N}^{-1}$) than in the South Pacific ($1 \times 10^{-2} \text{ Km}^2\text{N}^{-1}$). In addition, the sensitivity of DOC to the meridional wind stress is only notable near the eastern boundary of the Pacific, and both eastern and western

boundaries of the Atlantic (not shown). The sign of that sensitivity also alternates at different latitudinal belts.

3.2. DOC sensitivity to diffusivity

The DOC sensitivity to diapycnal diffusivities of temperature (K_t) is largely positive (Figures 5a-b), which seems to be in agreement with the result indicated in Tsujino et al. [2000]. The magnitude of the sensitivity is about 4 Ksm^{-2} in both the Pacific and Atlantic (Figure 5). In the Pacific (Figure 5a), the sensitivity is the strongest about 700 m, and becomes weaker towards the surface, the deeper ocean, and the higher latitudes. The strongest sensitivity is directly associated with the calculation of DOC being below 700 m. In the Atlantic (Figure 5b), the sensitivity distribution is slightly different from that in the Pacific: The strongest sensitivity is located at about 700 m in the North Atlantic subtropics near 15°N , and shifts upward to about 300 m in the South Atlantic subtropics near 30°S . The similarity is that the sensitivity also decreases towards the surface, deeper ocean, and higher latitudes as in the Pacific Ocean. In addition, there are weaker negative sensitivities near 800 m and 40°S (-1 Ksm^{-2}) and near 2 km between 40°S and 40°N (-0.5 Ksm^{-2}), and a weaker positive sensitivity below 2.5 km (1 Ksm^{-2}). Obviously, the DOC sensitivity to the diapycnal diffusivity is associated with the diapycnal diffusive heat flux, as will be discussed in detail in section 4.3.

In contrast with the strong DOC sensitivity to the diapycnal diffusivity of temperature, the sensitivity of DOC to the diapycnal diffusivity of salinity (K_s) is much smaller (not shown), since it does not directly contribute to the vertical heat fluxes although it can change the density and oceanic currents, and therefore make an indirect contribution to the vertical heat fluxes.

The contribution of the isopycnal diffusivity to DOC is different from that of the diapycnal diffusivities. The sensitivity of DOC to the isopycnal diffusivity for temperature and salinity (I_{ts}) is only noticeable in the South Pacific south of 50°S at a magnitude of $6 \times 10^{-7} \text{ Ksm}^{-2}$ (Figure 6a). In the South Atlantic, the DOC sensitivity is

about $-8 \times 10^{-7} \text{ Ksm}^{-2}$ south of 55°S , $8 \times 10^{-7} \text{ Ksm}^{-2}$ above 500 m between 60°S and 50°S (Figure 6b). The DOC sensitivity in other regions is negligible except for minor sensitivities near the northern boundary of the North Atlantic in Figure 6b. The reason is that there is a large slope of the isopycnal surface and thus large GM mixing. The detailed mechanism will be discussed in section 4.4.

3.3. Understanding DOC

Upon studying the adjoint sensitivity of DOC to the surface forcing and oceanic diffusivities, an interesting question we have not addressed is: Are these adjoint sensitivities relevant to the ocean dynamics and thermodynamics? First, the change of DOC below 700 m must be associated with the change of downward net heat flux across 700 m, although the net heat flux will eventually be balanced and becomes zero as indicated in Figure 3a. Secondly, the change of the net heat flux across 700 m will be associated with changes of vertical heat flux components as shown in (3). Therefore, the heat budget is analyzed using the adjoint model. The analysis of adjoint sensitivities of these heat flux components to those seven adjoint parameters may help understand the physics upon which the adjoint sensitivities are based.

To accomplish this goal, five additional adjoint runs were designed by setting the adjoint cost function to be the horizontally integrated net heat flux and its four components across 700 m, respectively, as indicated in (8). These five adjoint runs are also integrated for 500 years to reach a quasi-equilibrium state. However, we will present these adjoint sensitivities at year 100 in the following section, since the sensitivity of net heat flux always diminishes as the adjoint model reaches the quasi-equilibrium state.

4. Sensitivity of heat budget

4.1. Surface freshwater flux

The sensitivity of downward net heat flux (Q_{net}) at 700 m to the surface freshwater flux (E-P-R) is about 1 to $2 \times 10^{19} \text{ Jm}^{-1}$ in the Atlantic, about -0.5 to $-1 \times 10^{19} \text{ Jm}^{-1}$ in the Pacific, and about $-2 \times 10^{19} \text{ Jm}^{-1}$ in the Southern Ocean south of 50°S

(Figure 7a). The pattern of Q_{net} sensitivity is in good agreement with the pattern of DOC sensitivity shown in Figure 4a. Therefore, we have confidence that the DOC sensitivity is relevant to the ocean thermodynamics: In the Atlantic, when evaporation increases or precipitation decreases, the downward net heat flux across 700 m increases, and therefore DOC increases. The opposite situation occurs in the Pacific and Southern Ocean.

A further interesting question is: What contributes to the downward net heat flux change? To answer this question, we have examined the adjoint sensitivities of the four heat flux components as shown in Figures 7b-e. If evaporation increases, the advective heat flux (Q_w) increases in almost the entire ocean basins (Figure 7b) except for the northwest corner of the North Atlantic. The sensitivity of Q_w to E-P-R in the Atlantic is about 4 to $10 \times 10^{19} \text{ Jm}^{-1}$, which directly contributes to Q_{net} sensitivity (compare Figures 7a-b). The sensitivity of Q_w is about $2 \times 10^{19} \text{ Jm}^{-1}$ in the South Pacific and $1 \times 10^{19} \text{ Jm}^{-1}$ in the North Pacific, which is opposed by the negative sensitivity from GM mixing Q_{GM} (Figure 7e).

We suggest that Q_w increases because of the general enhancement of downward vertical velocity (W) due to denser surface water when E-P-R increases. Since Q_w is already downward, it increases as indicated in (6). This is consistent with the difference of sensitivity strength between the Pacific and Atlantic, since the temperature is higher in the Atlantic than in the Pacific at the same depth (see Figures 2a-b).

The sensitivity of diapycnal diffusive flux (Q_{DD}) to E-P-R also contributes largely to the sensitivity of Q_{net} in the Atlantic (compare Figures 7a and 7d). The magnitude of Q_{DD} sensitivity is about 2 to $4 \times 10^{19} \text{ Jm}^{-1}$ in both the Pacific and Atlantic except for near the northern boundaries of both the Pacific and Atlantic north of 40°N . The positive sensitivity is directly associated with the enhancement of vertical temperature stratification as shown in (4), since the vertical velocity anomaly is downward when E-P-R anomaly is positive. But, the temperature stratification is reduced instead of increased

in the North Atlantic north of 40°N where the convection is strong. Therefore, Q_{DD} sensitivity to E-P-R is negative (Figure 7d).

In the mean time, the strength of the overturning circulation increases when E-P-R increases in the Atlantic, according to the study of Bugnion [2001] under surface boundary condition (2). The reason may be that the surface water feeding into the overturning circulation in the Atlantic becomes denser. The strengthening of overturning circulation can enhance the vertical temperature stratification in regions of upwelling and eventually increase Q_{DD} . The situation in the Pacific is opposite to that in the Atlantic. The strengthening of overturning circulation with increasing E-P-R in the Atlantic seems to be consistent with the studies of Rahmstorf [1995; 1996] and Mikolajewicz and Voss [2000]. However, the study of Zhang et al. [1999] indicated that the overturning circulation in a model of the North Atlantic would be enhanced, as long as the difference of freshwater flux between the tropics and high latitudes increases: Either precipitation decreases in high latitudes, or evaporation decreases in the tropics.

On the other hand, as indicated in Figure 7e, the sensitivity of isopycnal diffusive flux (Q_{GM}) to E-P-R is negative almost over the entire ocean basin except for the North Atlantic north of 50°N . The magnitude of Q_{GM} sensitivity ranges from -2 to $-8 \times 10^{19} \text{ Jm}^{-1}$ in both the Pacific and Atlantic. This may again be because the increase of E-P-R enhances downwelling and thus the temperature stratification and the meridional temperature gradient on the isopycnal surface. Therefore, upward Q_{GM} increases as indicated in (5). In the Southern Ocean, the dominant effect may be that the enhancement of convection due to the increase of E-P-R results in a steeper slope of the isopycnal surface. Therefore, the upward Q_{GM} strengthens and DOC weakens. However, in the North Atlantic north of 50°N where convection is very active, the enhancement of E-P-R increases the temperature in the deep ocean, which results in a reduction of meridional temperature gradient and upward Q_{GM} .

Comparison of the sensitivity patterns of Q_{net} and Q_{GM} in Figures 7a and 7e shows that the negative sensitivity of Q_{GM} directly contributes to the negative sensitivity of Q_{net} and DOC in the Pacific and Southern Ocean as shown in Figure 4a. However, the negative sensitivity over the Atlantic between 50°S and 50°N is less than compensated by the sensitivities from vertical advective heat flux Q_w and diapycnal diffusive heat flux Q_{DD} . In addition, the sensitivity of convective heat flux (Q_{CV}) is negative and weak although it is relatively strong in the North Atlantic at a magnitude of $-2 \times 10^{19} \text{ Jm}^{-1}$ (Figure 7c). Q_{CV} does not contribute very much to Q_{net} or DOC sensitivity.

In short, in the case of a positive E-P-R anomaly, the downward advective heat flux and diapycnal diffusive heat flux increase in the Atlantic due to enhancing downward vertical velocity, overturning circulation, and temperature stratification. Therefore, DOC increases. In the Pacific and Southern Ocean, a positive E-P-R anomaly increases the meridional temperature gradient (Figure 7a) and slope of the isopycnal surface, and therefore increases the upward GM mixing that results in the decrease of DOC. These mechanisms are shown schematically in Figure 8.

4.2. Net surface heat flux

The DOC sensitivity to the net surface heat flux (Q_s) is closely associated with the sensitivity of net heat flux (Q_{net}) at 700 m as a comparison of Figures 4b and 9a shows. The Q_{net} sensitivity is only notable in the North Atlantic north of 40°N at a magnitude of 2 to $8 \times 10^9 \text{ m}^2$, and in the Southern Ocean south of 50°S at a magnitude of $8 \times 10^9 \text{ m}^2$.

The positive sensitivity of Q_{net} in the North Atlantic north of 40°N (Figure 9a) is caused by the vertical advective heat flux (Q_w) as indicated in Figure 9b, which is at a magnitude of $10 \times 10^9 \text{ m}^2$. This can be simply explained by most of the heat anomaly being absorbed by the deeper ocean as indicated in the study of Huang and Liu [2001]. As a result, the temperature near 700 m and downward Q_w increase according to (6), which increases DOC. Figure 10 shows schematically the hypothesized physical

processes. Note that the increase in Q_w does not necessarily imply an increase in the vertical velocity (W). Other studies in fact show that W and meridional overturning circulation are reduced if Q_s increases [Bugnion, 2001; Mikolajewicz and Voss, 2000; and Weaver et al., 1993]. In addition, the heat fluxes of convection (Q_{CV}) and GM mixing (Q_{GM}) also contribute partly to the positive sensitivity of Q_{net} and DOC in the North Atlantic north of 40°N as indicated in Figures 9c and 9e in this area.

In the Southern Ocean south of 50°S , it is very clear that the sensitivity of Q_{net} is exclusively associated with Q_{GM} (compare Figures 9a and 9e). The magnitude of Q_{GM} sensitivity to Q_s is about $10 \times 10^9 \text{ m}^2$. The reason resulting in this positive sensitivity might be that, for a given downward Q_s anomaly, the temperature along the Antarctic Circumpolar Ocean increases due to the penetration of surface heat flux by convection and absorption by the deeper ocean. This leads to the decrease of meridional temperature gradient and flattening of the isopycnal surface, which favor the decrease of upward Q_{GM} and the increase of DOC according to (5). These processes are also indicated schematically in Figure 10. In addition, there is a negative Q_{GM} sensitivity to Q_s between 45°S and 55°S at a magnitude of -5 to $-10 \times 10^9 \text{ m}^2$. The negative sensitivity of Q_{GM} contributes directly to the sensitivity of Q_{net} at 700 m and DOC in the South Atlantic as indicated in Figures 9a and 9e. This might be associated with downward heat transport by the downward branch of the Deacon Cell in Figure 1b. The heating due to Q_s may reduce the meridional circulation within the Deacon Cell, which may generate a negative anomaly of temperature and a positive anomaly of meridional temperature gradient. This positive anomaly would then enhance Q_{GM} (see equation 5) and DOC may decrease.

4.3. Diapycnal diffusivity of temperature

As shown in Figures 4-5, the adjoint sensitivities to diffusivities in the Pacific are somewhat similar to those in the Atlantic. Therefore we will focus on the mechanisms in the Atlantic in this and the following sections 4.3 and 4.4.

The sensitivity of net heat flux (Q_{net}) at 700 m to the diapycnal diffusivity of temperature (K_t) is in agreement with DOC sensitivity in the Atlantic. As shown in Figure 11a, the sensitivity of Q_{net} exhibits a maximum of $6 \times 10^{14} \text{ Jm}^{-2}$ near 10°N and 700 m. The maximum Q_{net} sensitivity shifts upward to 300 m in the South Atlantic at 30°S . The Q_{net} sensitivity becomes weaker in the upper and lower ocean, and towards higher latitudes. A weak Q_{net} sensitivity of $2 \times 10^{14} \text{ Jm}^{-2}$ is found below 2.5 km. In addition, there is a weak negative sensitivity of Q_{net} near 2 km between 40°S and 30°N . A negative Q_{net} sensitivity of $-2 \times 10^{14} \text{ Jm}^{-2}$ also contributes to DOC sensitivity near 700 m and 40°S . These characteristics of Q_{net} sensitivity are entirely coherent with the DOC sensitivity shown in Figure 5b.

When we look into the possible contributors to Q_{net} sensitivity, it is very clear that the sensitivity of diapycnal diffusive heat flux (Q_{DD}) to K_t (Figure 11d) dominates the sensitivities of Q_{net} and DOC in the Atlantic. Consistent with the distribution of Q_{net} sensitivity (Figure 11a), the sensitivity of Q_{DD} exhibits a maximum of $6 \times 10^{15} \text{ Jm}^{-2}$ near 20°N and 700 m, and shifts upward to 400 m at 25°S . Since K_t is directly associated with Q_{DD} as shown in (4), it is easy to understand why the diapycnal diffusivity of temperature is a major factor affecting Q_{net} through Q_{DD} .

The contributions from vertical advection (Q_w), convection (Q_{CV}), and GM mixing (Q_{GM}) are either very weak or in the opposite sign to Q_{net} sensitivity (Figures 11b, 11c, and 11e), even though the strength of the meridional overturning circulation is generally increased by an increase of K_t in the tropics and subtropics [Bugnion, 2001; Marotzke, 1997]. The exception is that a negative Q_{GM} sensitivity of $-2 \times 10^{15} \text{ Jm}^{-2}$ seems to contribute to the sensitivities of Q_{net} and DOC near 45°S and 700 m. This can be explained by an increase of meridional temperature gradient, since Q_{DD} is relatively larger in lower latitudes due to stronger temperature stratification (see Figures 2a-b). Therefore, the meridional temperature gradient increases, which results in a negative sensitivity of Q_{GM} since the gradient is negative as indicated in (5) and shown in Figure

11e. The association between the sensitivities of Q_{GM} and Q_{DD} can be seen clearly from their well correlated spatial pattern shown in Figures 11d and 11e.

4.4. Isopycnal diffusivity

The sensitivity pattern of downward net heat flux (Q_{net}) at 700 m to the isopycnal diffusivity for temperature and salinity (I_{ts}) matches perfectly with that of DOC in the South Atlantic (compare Figures 12a and 6b). The magnitude of Q_{net} sensitivity is about $-10 \times 10^7 \text{ Jm}^{-2}$ south of 55°S , $8 \times 10^7 \text{ Jm}^{-2}$ above 500 m between 60°S and 50°S . The sensitivity of Q_{net} is negligible in other regions except near 60°N below 1 km where there are a positive and a negative sensitivity in a small area.

Comparing the pattern of Q_{net} sensitivity to I_{ts} (Figure 12a) with the sensitivities of its four components (Figures 12b-e), we find that the sensitivity of GM mixing (Q_{GM}) dominates the Q_{net} sensitivity (compare Figures 12a and 12e) and DOC sensitivity south of 40°S . The sensitivity of Q_{GM} is about $-3 \times 10^8 \text{ Jm}^{-2}$ south of 55°S , about $2 \times 10^8 \text{ Jm}^{-2}$ above 500 m between 60°S and 50°S . The distribution of Q_{GM} sensitivity agrees well with the distribution of Q_{net} sensitivity south of 40°S . The sensitivities from the other three components are either weak (Q_w and Q_{CV} sensitivities in Figures 12b and 12c) or have the opposite sign (Q_{DD} sensitivity in Figure 12d) to Q_{net} sensitivity. We note that the isopycnal diffusivity for temperature and salinity (I_{ts}) does nevertheless appear to have a large impact on the meridional overturning circulation in the region of the Gulf Stream [Bugnion, 2001].

The cause of the negative Q_{GM} sensitivity south of 55°S seems to be straightforward. In that region, the meridional temperature gradient is positive and the slope of the isopycnal surface is negative. According to (5), an increase in I_{ts} would indeed normally lead to a decrease in Q_{GM} . However, the Q_{GM} sensitivity to I_{ts} becomes positive in the region above 500 m between 60°S and 50°S . This may be because the slope of the isopycnal surface is reduced due to GM mixing in the meridional direction:

$$Q_{GM}^Y = -\iint I_{ts} \frac{\partial T}{\partial y} dx dz . \quad (9)$$

This would cause the upward Q_{GM} in (5) to decrease. Figure 13 presents schematically the mechanisms associated with I_{ts} and DOC.

In the South Pacific south of 40°S, the negative sensitivity (Figure 6a) is primarily controlled by a Q_{GM} sensitivity that is directly associated with I_{ts} as indicated in (5) (not shown).

5. Uncertainty of DOC and Q_{net}

As stated in our introduction, the world ocean largely controls how rapidly climate changes due to its tremendous heat capacity (DOC). Consequently, projections of global warming depend on climate models being able to simulate the heat uptake accurately [Barnett et al., 2001]. Our estimates of the sensitivity of the heat uptake to model input parameters can give us insight into why the models differ so wildly in their simulations of heat uptake [Forest et al., 2002], and into the uncertainty of oceans in regulating our climate. Furthermore, we can compare the different sources of uncertainty to see which are the most important.

According to our adjoint sensitivity defined in (7), the uncertainties of DOC and Q_{net} can be calculated, respectively, as

$$\delta \bar{T}_n = \pm \sum_{i,j,k} \left| \frac{\partial \bar{T}}{\partial P_n} \right| \times |\delta P_n|, \quad n = 1, N. \quad (10)$$

$$\delta \bar{Q}_n = \pm \sum_{i,j,k} \left| \frac{\partial \bar{Q}_{net}}{\partial P_n} \right| \times |\delta P_n|, \quad n = 1, N. \quad (11)$$

Here δP_n is the error bar of adjoint parameter P_n . The estimate of DOC and Q_{net} uncertainties is likely to be an overestimate owing to the absolute sign. To estimate the uncertainties of DOC and Q_{net} according to our adjoint sensitivity, we need to know the

error bars of our adjoint parameters. Based on Schmitt et al. [1989], the error bar of net surface heat flux (Q_s) is about 30 Wm^{-2} , which is about 25% of its climatology. The error bar of E-P-R is about 30-40 cm per year, which is about 30% of its climatology according to the study of Isemer and Hasse [1991]. The error bar of wind stress is about 0.03 Nm^{-2} , which is about 30% of its climatology based on Isemer and Hasse [1991]. Since the meridional wind stress τ_y is set to be zero in our model, we use $\tau_y = 0.2\tau_x$ to estimate the DOC uncertainty caused by τ_y . The error bar of ocean diffusivities is probably even larger than that of the surface forcing. Estimates of diapycnal diffusivities (K_t, K_s) range from 10^{-5} to $10^{-4} \text{ m}^2\text{s}^{-1}$ [Ledwell et al., 2000; Ledwell and Hickey, 1995; Ledwell and Bratkovich, 1995; Polzin et al., 1997]. Estimates of isopycnal diffusivity (I_{ts}) range from 1×10^3 to $7 \times 10^3 \text{ m}^2\text{s}^{-1}$ according to Zhang et al. [2001]. Based on these studies, we take 30% surface forcing and 50% diffusivities as their error bars in our estimate of DOC and Q_{net} . The result is calculated according to (10) and (11), and shown in the second and third columns of Table 1.

The estimated uncertainty of DOC in Table 1 (second column) indicates that the uncertainty from I_{ts} has the largest contribution of 0.7°K . The uncertainty from K_t is 0.4°K . The E-P-R contributes to the DOC uncertainty about 0.3°K . The uncertainties from $Q_s, \tau_x, \tau_y,$ and K_s are about 0.1°K . We need to note that the DOC uncertainty of 1°K represents a heat capacity of about $3.7 \times 10^{24} \text{ J}$ for our model ocean or $1.6 \times 10^{10} \text{ Jm}^{-2}$. It would take about 125 years for the forcing from a doubling of carbon dioxide (4 Wm^{-2}) to accumulate this much energy. The effect of surface freshwater flux on DOC and overturning circulation seems to be dominant over that of surface heat flux. This is consistent with Weaver et al. [1993] in a study of the thermohaline circulation. However, the sensitivity study of Mikolajewicz and Voss [2000] indicated that the surface heat flux might be as important as the surface fresh water flux to the thermohaline circulation.

In addition, we have to note that these uncertainties are not uniformly distributed over the global ocean: The uncertainty from I_{ts} occurs in the Southern Ocean south of

40°S (Figure 6). The uncertainty from K_t is found in the large area of the tropics and subtropics in both the Atlantic and Pacific (Figure 5). The uncertainty from E-P-R occurs mainly in the Atlantic tropics and subtropics (Figure 4a). The uncertainty from Q_s occurs mainly in the North Atlantic north of 40°N, and the Southern Ocean south of 50°S. The uncertainty from τ_x is largely found in the South Atlantic and South Pacific. We also need to note that our estimate of DOC uncertainty depends very much on the error bars of our adjoint parameters. The error bars of these parameters need to be confirmed further. Especially, the 50% error bar of diffusivities may still be too small. On the other hand, our estimate in (10) and (11) is likely to be an overestimate, since the uncertainty from different regions in reality may partially cancel. The magnitude of Q_{net} uncertainty is consistent with DOC uncertainty, and ranges from 0.01 to 0.22 PW (1 $PW = 10^{15} W$) as illustrated in the third column of Table 1.

6. Summary

The adjoint sensitivity and uncertainty of DOC from seven parameters at the time scale 500 years were studied using the MIT OGCM and its adjoint. These parameters are the surface freshwater flux, downward net surface heat flux, zonal and meridional wind stress, and diapycnal and isopycnal diffusivities of temperature and salinity. The physical mechanisms are explored using adjoint sensitivities of downward heat fluxes (Q_{net} and its four components) into the deep ocean below 700 m at the time scale of 100 years.

Our study indicates that DOC and Q_{net} are sensitive to the isopycnal diffusivity for temperature and salinity, and sensitive to the diapycnal diffusivity of temperature, but less sensitive to the diapycnal diffusivity of salinity. The DOC uncertainty is about 0.7°K from isopycnal diffusivity for temperature and salinity, diapycnal diffusivity of temperature. DOC and Q_{net} are also sensitive to the surface freshwater flux, zonal wind stress, and downward net surface heat flux. The DOC uncertainty is about 0.3°K owing to the surface freshwater flux, and about 0.1°K owing to the zonal wind stress and downward net surface heat flux. The uncertainty and sensitivity of Q_{net} are very coherent

with those of DOC. These uncertainties represent estimates of the relative importance of the different factors in affecting the ocean heat uptake in coarse resolution GCMs.

The DOC sensitivity to the diapycnal diffusivity of temperature occurs mainly in the tropics and subtropics in both the Pacific and Atlantic. The sensitivity is largely positive, and its maximum is found near the level below which DOC is calculated. The sensitivity decreases towards the upper and lower ocean, and towards lower and higher latitudes. The change of DOC owing to diapycnal diffusivity of temperature is primarily associated with the diapycnal diffusive heat flux, which is reasonable and consistent with intuition. The DOC increases when the diapycnal diffusivity increases.

The DOC sensitivities to the isopycnal diffusivity for temperature and salinity are very important. The sensitivity distribution in the Pacific is similar to that in the Atlantic. All these sensitivities are found dominantly in the Antarctic Circumpolar Ocean, where the slope of the isopycnal surface is large and GM mixing is the strongest. The change of DOC owing to isopycnal diffusivity is largely associated with the heat flux due to GM mixing. These conclusions seem to be mutually consistent.

The DOC sensitivity to the surface freshwater flux is positive in the Atlantic, but negative in the Pacific and Antarctic Circumpolar Ocean. When evaporation increases, the DOC below 700 m increases in the Atlantic but decreases in the Pacific. The change of DOC owing to the freshwater flux is associated with downward velocity and temperature stratification in the Pacific and Atlantic, but associated with convection, the slope of the isopycnal surface, and GM mixing in the Antarctic Circumpolar Ocean. The change of overturning circulation due to the surface freshwater flux may also have contributed to the change of temperature stratification. Our conclusion is consistent with other studies in the Atlantic [Bugnion, 2001; Rahmstorf, 1996 and 1995].

The DOC sensitivity to the net surface heat flux is largely positive, and only notable in the North Atlantic north of 40°N and in the Antarctic Circumpolar Ocean. The DOC increases when downward net surface heat flux increases in these areas. In the

North Atlantic, the change of DOC owing to the surface heat flux is mainly associated with vertical advective heat flux through the increase of ocean temperature near 700 m. But, it is associated with the GM mixing through the reduction of meridional temperature gradient and the enhancement of the slope of the isopycnal surface in the Antarctic Circumpolar Ocean. It seems that the heat flux can only penetrate into the deep ocean in the higher latitudes, which agrees with the previous study of Huang and Liu [2001].

For a perturbation of net surface flux in the tropical and subtropical regions, it cannot penetrate into the deep ocean. It does not seem to be transported to the higher latitudes either. Otherwise, it will eventually modify the DOC as the local perturbation does. The only possibility is that the perturbation is damped by the relaxation of SST as indicated in (1). This may also explain why the DOC is sensitive to E-P-R over the entire basin, since its perturbation in the lower latitudes could be advected to the higher latitudes without damping out under the flux boundary condition (2). The effect of the surface boundary conditions (1) and (2) was also noted by Bugnion [2001] and Huang [1993], and further study is on the way.

We did not discuss the mechanism of DOC sensitivity to the zonal wind stress, although its sensitivity and associated uncertainty are not trivial if it is compared with other parameters in Table 1. As indicated by Bugnion [2001], Toggweiler and Samuel [1995], Tsujino and Suginozara [1999], and Hasumi and Suginozara [1999], the zonal wind stress and its associated Ekman pumping may have a large contribution to the overturning circulation. However, much of this sensitivity disappears if the ocean is coupled to a simple atmospheric model [Bugnion, 2001]. Also, a careful analysis indicates that the pattern of wind stress does not match that of DOC sensitivity very well. In addition, the pattern of DOC sensitivity in the Pacific is very different from that in the Atlantic as indicated in Figure 4c, although the wind stress does not exhibit large difference. We expect further study to be done to clarify the effect of surface wind stress on the deep ocean circulation and heat content.

Our results from the adjoint sensitivity analysis indicate that the DOC sensitivities at the time scale of 500 years are consistent with those at the time scale of 1000 years, as shown in the fourth column of Table 1. But, their values change largely, indicating that the adjoint calculation has not reached its equilibrium. The sensitivities of DOC below 200 m at the time scale of 500 years also seem to be consistent with those below 700 m as indicated in the fifth column of Table 1. Of course, the actual sensitivity of heat content below 200 m is larger than that below 700 m, although their mean temperature sensitivity is similar as presented in Table 1.

Finally, we need to note that our sensitivity study is based on the adjoint OGCM that is not coupled with the atmosphere. Therefore, it is not clear whether our conclusions about the sensitivities to surface fluxes would be robust in the coupled ocean atmosphere system. In a coupled system, these fluxes will be modified in non-uniform ways. However, since the diffusivities are specified in ocean GCMs independently of whether they are coupled to an atmosphere, our results for these sensitivities are more likely to apply to a coupled system. In particular, our results suggest that the heat uptake by the deep oceans and the DOC are sensitive to both the diapycnal thermal diffusivity and the isopycnal diffusivity.

Acknowledgements

We thank Drs. Alistair Adcroft and Patrick Heimbach for helping setup the MIT OGCM. Discussions with Drs. Veronique Bugnion, Chris Forest, Jochem Marotzke, and Andrei Sokolov were a great help in the early stage of our study. The comments from two anonymous reviewers gave many improvements in the final version of the manuscript.

References

- Barnett, T. P., D. W. Pierce, and R. Schnur, Detection of anthropogenic climate change in the world's ocean, *Science*, 292, 270-274, 2001.
- Bryan, F., Parameter sensitivity of primitive equation ocean general circulation models, *J. Phys. Oceanogr.*, 17, 970-985, 1986.
- Bryan, K., Ocean circulation models, in Strategies for Future Climate Research, edited by M. Latif, pp. 265-286, Max-Planck-Institut für Meteorologie, Hamburg, Germany, 1991.
- Bugnion, V., *Driving the ocean's overturning: Analysis with adjoint models*, Ph.D. dissertation, Massachusetts Institute of Technology, 179 pp., 2001, available at Lindgren Library, MIT Building 54, 77 Massachusetts Ave., Cambridge, MA-02139.
- Cummins, P. F., G. Holloway, and A. E. Gargett, Sensitivity of the GFDL ocean general circulation model to a parameterization of vertical diffusion, *J. Phys. Oceanogr.*, 20, 817-830, 1990.
- Danabasoglu, G., and J. C. McWilliams, Sensitivity of the global ocean circulation to parameterizations of mesoscale tracer transport, *J. Clim.*, 8, 2967-2987, 1995.
- da Silva, A. M., C. C. Young, and S. Levitus, *Atlas of surface marine data 1994, Volume, Anomalies of directly observed quantities*, NOAA Atlas NESDIS 7, 416 pp., 1994.
- Duffy, P. B., K. Caldeira, J. Selvaggi, and M. I. Hoffert, Effects of subgrid-scale mixing parameterizations on simulated distributions of natural ¹⁴C, temperature, and salinity in a three-dimensional ocean general circulation model, *J. Phys. Oceanogr.*, 27, 498-523, 1997.

- Forest, C. E., M. R. Allen, P. H. Stone, A. P. Sokolov, M. R. Allen, and M. D. Webster, Quantifying uncertainties in climate system properties with the use of recent climate observations, *Science*, 295, 113-117, 2002.
- Gent, P. R., and J. C. McWilliams, Isopycnal mixing in ocean circulation model, *J. Phys. Oceanogr.*, 20, 150-155, 1990.
- Gent, P.R., and J. Willebrand, T. J. McDougall, and J. C. McWilliams, Parameterizing eddy-induced tracer transports in ocean circulation models, *J. Phys. Oceanogr.*, 25, 463-474, 1995.
- Gerdes, R., C. Koberle, and J. Willebrand, The influence of numerical advection schemes on the results of ocean general circulation models, *Clim. Dyn.*, 5, 211-226, 1991.
- Giering, R., and T. Kaminski, Recipes for adjoint code construction, *Trans. Math. Software*, 24, 437-474, 1998.
- Giering, R., *Tangent linear and adjoint model compiler, Users manual*, Max-Planck Institut, Hanburg, Germany, 64 pp., 1999.
- Goose, H., E. Deleersnijder, T. Fichefet, and M. H. England, Sensitivity of a global coupled ocean sea-ice model to the parameterization of vertical mixing, *J. Geophys. Res.*, 104, 13,681-13,695, 1999.
- Gregory, J. M., Vertical heat transports in the ocean and their effect on time-dependent climate change, *Climate Dyn.*, 16, 501-515, 2000.
- Griffies, S. M., The Gent-McWilliams skew flux, *J. Phys. Oceanogr.*, 28, 831-841, 1998.
- Griffies, S. M., A. Gnanadesikan, R. C. Pacanowski, V. D. Larichev, J. K. Duknowicz, and R. D. Smith, Isonutral diffusion in a z-coordinate ocean model, *J. Phys. Oceanogr.*, 28, 805-830, 1998.
- Hasumi, H., and N. Suginoara, Atlantic deep circulation controlled by heating in the Southern Ocean, *Geophys. Res. Let.*, 26, 1873-1876, 1999.
- Hellerman, S., and M. Rosenstein, Normal monthly wind stress over the world with error estimate, *J. Phys. Oceanogr.*, 13, 1093-1104, 1983.

- Hu, D., On the sensitivity of thermocline depth and meridional heat transport to vertical diffusivity in OGCMs, *J. Phys. Oceanogr.*, 26, 1480-1494, 1996.
- Huang, B., and Liu Z., Temperature trend of the last 40 yr in the upper Pacific Ocean, *J. Clim.*, 14, 3738-3750, 2001.
- Huang, R., Real freshwater flux as a natural boundary condition for the salinity balance and thermohaline circulation forced by evaporation and precipitation, *J. Phys. Oceanogr.*, 23, 2428-2446, 1993.
- Huang, R., and R. L. Chou, Parameter sensitivity study of the saline circulation, *Clim. Dyn.*, 9, 391-409, 1994.
- Isemer, H. J., and L. Hasse, The scientific Beaufort equivalent scale: Effects on wind statistics and climatological air-sea flux estimates in the North Atlantic Ocean, *J. Clim.*, 4, 819-836, 1991.
- Jenkins, W. J., Determination of isopycnal diffusivity in the Sargasso Sea, *J. Phys. Oceanogr.*, 21, 1058-1061, 1991.
- Jiang, S., P. H. Stone, and P. Malanotte-Rizzoli, An assessment of the Geophysical Fluid Dynamics Laboratory ocean model with coarse resolution: Annual-mean climatology, *J. Geophys. Res.*, 104, 25,623-25,645, 1999.
- Kalnay, E., S. K. Park, Z. X. Pu, and J. Gao, Application of the quasi-inverse method to data assimilation, *Mon. Wea. Rev.*, 128, 864-875, 2000.
- Kamenkovich, I. V., A. Sokolov, and P. H. Stone, A coupled atmospheric-ocean model of intermediate complexity for climate change, *Clim. Dyn.*, 2002, accepted.
- Kamenkovich, I. V., and P. J. Goodman, The dependence of AABW transport in the Atlantic on vertical diffusivity, *Geophys. Res. Lett.*, 27, 3739-3742, 2000.
- Large, W. G., G. Danabasoglu, S. C. Doney, and J. C. McWilliams, Sensitivity to surface forcing and boundary layer mixing in a global ocean model: Annual-mean climatology, *J. Phys. Oceanogr.*, 27, 2418-2447, 1997.

- Ledwell, J. R., E. T. Montgomery, K. L. Polzin, L. C. St. Laurent, R. W. Schmitt, and J. M. Toole, Evidence for enhanced mixing over rough topography in the abyssal ocean, *Nature*, 403, 179-182, 2000.
- Ledwell, J. R., and B. M. Hickey, Evidence for enhanced boundary mixing in the Santa Monica Basin, *J. Geophys. Res.*, 100, 20,665-20,679, 1995.
- Ledwell, J. R., and A. Bratkovich, A tracer study of mixing in the Santa Cruz Basin, *J. Geophys. Res.*, 100, 20,681-20,704, 1995.
- Levitus, S., J. I. Antonov, T. P. Boyer, and C. Stephens, Warming of the world ocean, *Science*, 287, 2225-2229, 2000.
- Levitus, S., J. I. Antonov, J. Wang, T. L. Delworth, K. W. Dixon, and A. J. Broccoli, Anthropogenic warming of earth s climate system, *Science*, 292, 267-270, 2001.
- Levitus, S., and T. P. Boyer, *World ocean atlas 1994, Volume 4: Temperature*, NOAA Atlas NESDIS, 117 pp., U. S. Department of Commerce, Washington D.C., 1994.
- Levitus, S., R. Burgett, and T. P. Boyer, *World ocean atlas 1994, Volume 3: Salinity*, NOAA Atlas NESDIS 3, 99 pp., U. S. Department of Commerce, Washington D.C., 1994.
- Marotzke, J., Boundary mixing and dynamics of three-dimensional thermohaline circulations, *J. Phys. Oceanogr.*, 27, 1713-1728, 1997.
- Marotzke, J., R. Giering, K. Q. Zhang, D. Stammer, C. Hill, and T. Lee: Construction of the adjoint MIT ocean general model and application to Atlantic heat transport sensitivity, *J. Geophys. Res.*, 104, 29,529-29,547, 1999.
- Mashall, J., A. Adcroft, C. Hill, L. Perelman, and C. Heisey, A finite volume, incompressible Navier Stokes model for studies of the ocean on parallel computers, *J. Geophys. Res.*, 102, 5753-5766, 1997a.
- Mashall, J., C. Hill, L. Perelman, and A. Adcroft, Hydrostatic, quasi-hydrostatic and nonhydrostatic ocean modeling, *J. Geophys. Res.*, 102, 5733-5752, 1997b.

- Mashall, J. H. Jones, and C. Hill, Efficient ocean modeling using non-hydrostatic algorithms, *J. Marine System*, 18, 115-134, 1998.
- Mikolajewicz, U. M., and R. Voss, The role of the individual air-sea flux components in CO₂-induced changes of the ocean s circulation and climate, *Clim. Dyn.*, 16, 627-642, 2000.
- Nakamura, M., and Y. Cao, On the eddy isopycnal thickness diffusivity of the Gent-McWilliams subgrid mixing parameterization, *J. Clim.*, 13, 502-510, 2000.
- Pierce, D. W., T. P. Barnett, and U. Mikolajewicz, Competing roles of heat and freshwater flux in forcing the thermohaline oscillation, *J. Phys. Oceanogr.*, 25, 2046-2064, 1995.
- Polzin, K. L., J. M. Toole, J. R. Ledwell, and R. W. Schmitt, Spatial variability of turbulent mixing in the abyssal ocean, *Science*, 276, 93-96, 1997.
- Rahmstorf, S., On the freshwater forcing and transport of the Atlantic thermohaline circulation, *Clim. Dyn.*, 12, 799-811, 1996.
- Rahmstorf, S., Bifurcation of the Atlantic thermohaline circulation in response to changes in the hydrological cycle, *Nature*, 378, 145-149, 1995.
- Redi, M. H., Oceanic isopycnal mixing by coordinate rotation, *J. Phys. Oceanogr.*, 12, 1154-1158, 1982.
- Scott, J. R., and Marotzke, Diapycnal stirring and meridional overturning circulation: Does it matter where the mixing occurs? Submitted to *J. Phys. Oceanogr.*, 2001.
- Sun, Fengying, *Water exchange between the subpolar and subtropical North Pacific Ocean*, MS Thesis, University of Wisconsin-Madison, 62pp., 2000, Available at Schwerdtfeger Library, 1225 W. Dayton St., Madison, WI-53706.
- Toggweiler, J. R., and B. Samuels, Effect of Drake Passage on the global thermohaline circulation, *Deep-Sea Res.*, 42, 477-500, 1995.

- Trenberth, K. E., J. G. Olson, and W. G. Large, *A global ocean wind stress climatology based on ECMWF analysis*, Tech Note NCAR/TN-338+STR, Nat. Cent. for Atmos. Res., Boulder, Colo., 1989.
- Tsujino, H., H. Hasumi, and N. Sugimoto, Deep Pacific circulation controlled by vertical diffusivity at the lower thermocline depths, *J. Phys. Oceanogr.*, *30*, 2853-2865, 2000.
- Tsujino, H., and N. Sugimoto, Thermohaline circulation enhanced by wind forcing, *J. Phys. Oceanogr.*, *29*, 1506-1516, 1999.
- Waelbroeck, C., and J. F. Louis, Sensitivity analysis of a model of CO₂ exchange in tundra ecosystems by the adjoint method, *J. Geophys. Res.*, *100*, 2801-2816, 1995.
- Weaver, A., J. Marotzke, P. E. Cummins, and E. S. Sarachik, Stability and variability of the thermohaline circulation, *J. Phys. Oceanogr.*, *23*, 39-60, 1993.
- Winguth, A. M. E., D. Archer, E. Maier-Reimer, and U. Mikolajewicz, *Paleonutrient data analysis of the glacial Atlantic using an adjoint ocean general circulation model*, Max-Planck-Institut für Meteorologie, Reports No. 281, 20 pp., 1998.
- Yu, L., and P. Malanotte-Rizzoli, Inverse modeling of seasonal variations in the North Atlantic Ocean, *J. Phys. Oceanogr.*, *28*, 902-922, 1998.
- Zaucker, F., T. F. Stocker, and W. S. Broecker, Atmospheric freshwater fluxes and their effect on the global thermohaline circulation, *J. Geophys. Res.*, *99*, 12,443-12,457, 1994.
- Zhang, H. M., M. D. Prater, T. Rossby, Isopycnal Lagrangian statistics from North Atlantic Current RAFOS float observations, *J. Geophys. Res.*, *106*, 13,817-13,836, 2001.
- Zhang, J., R. W. Schmitt, R. X. Huang, The relative influence of diapycnal mixing and hydrological forcing on the stability of the thermocline circulation, *J. Phys. Oceanogr.* *29*, 1096-1108, 1999.

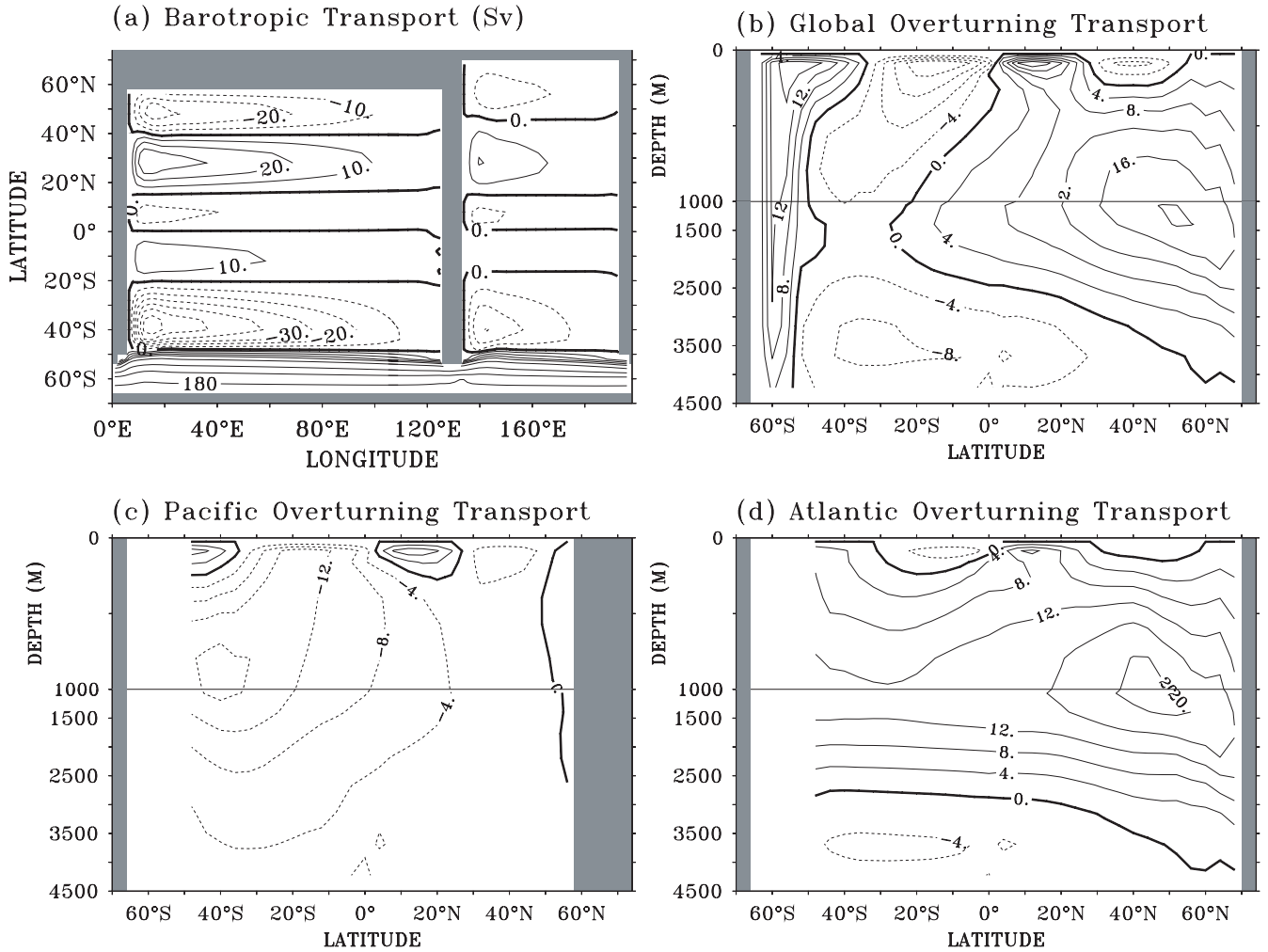


Figure 1. (a) Barotropic stream function, contour interval (CI) is 10 Sv between -60 and 60 , and 40 Sv between 60 and 180 . (b) Global, (c) Pacific, and (d) Atlantic overturning stream function, CI is 4 Sv. The streamlines near the northern and southern boundaries are clipped due to smoothing applied in plotting. Positive (negative) values are represented with solid (dashed) contours.

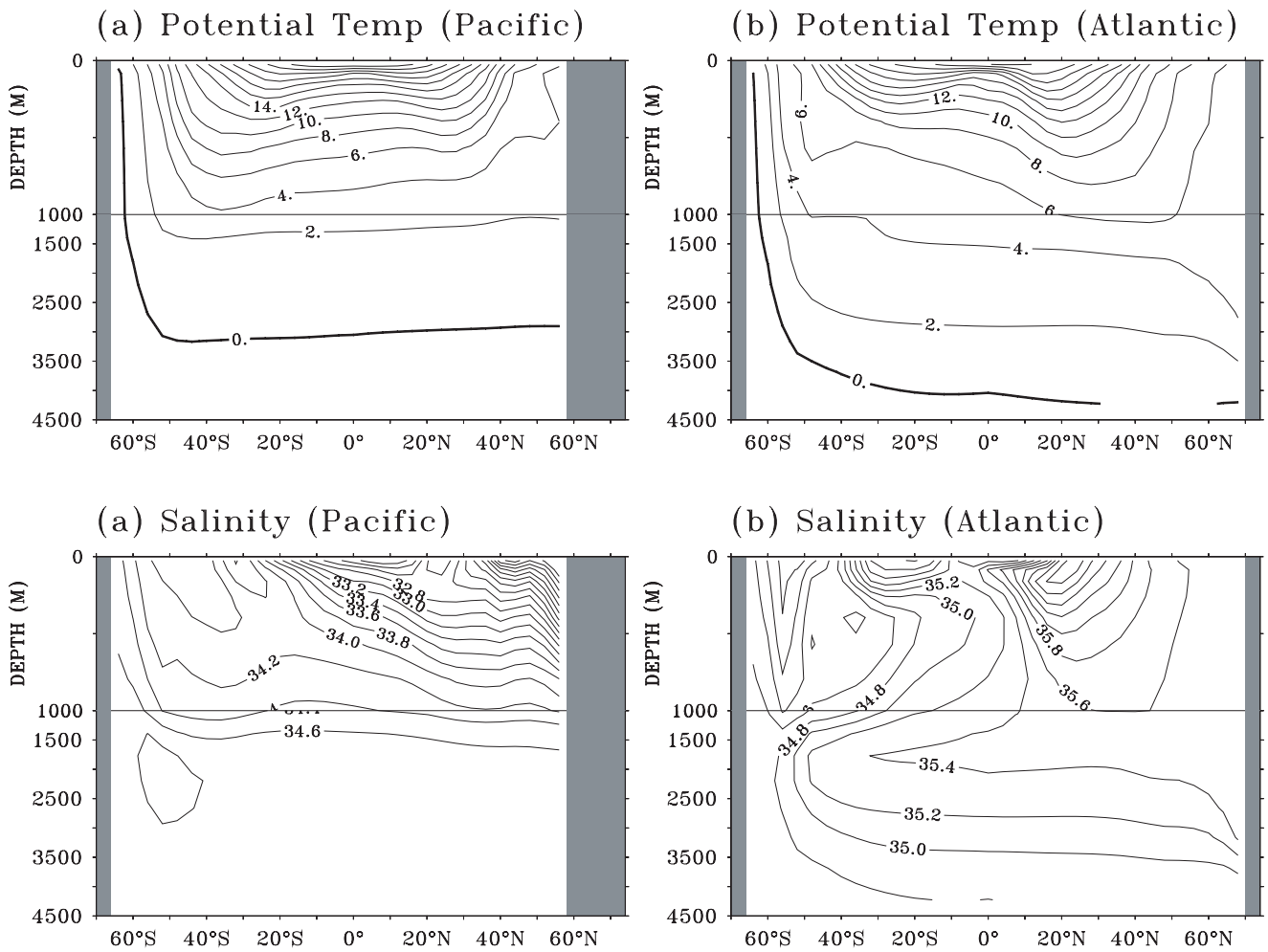


Figure 2. Zonal averaged potential temperature in the (a) Pacific and (b) Atlantic, CI is 2°C, and salinity in the (a) Pacific and (b) Atlantic, CI is 0.2 psu.

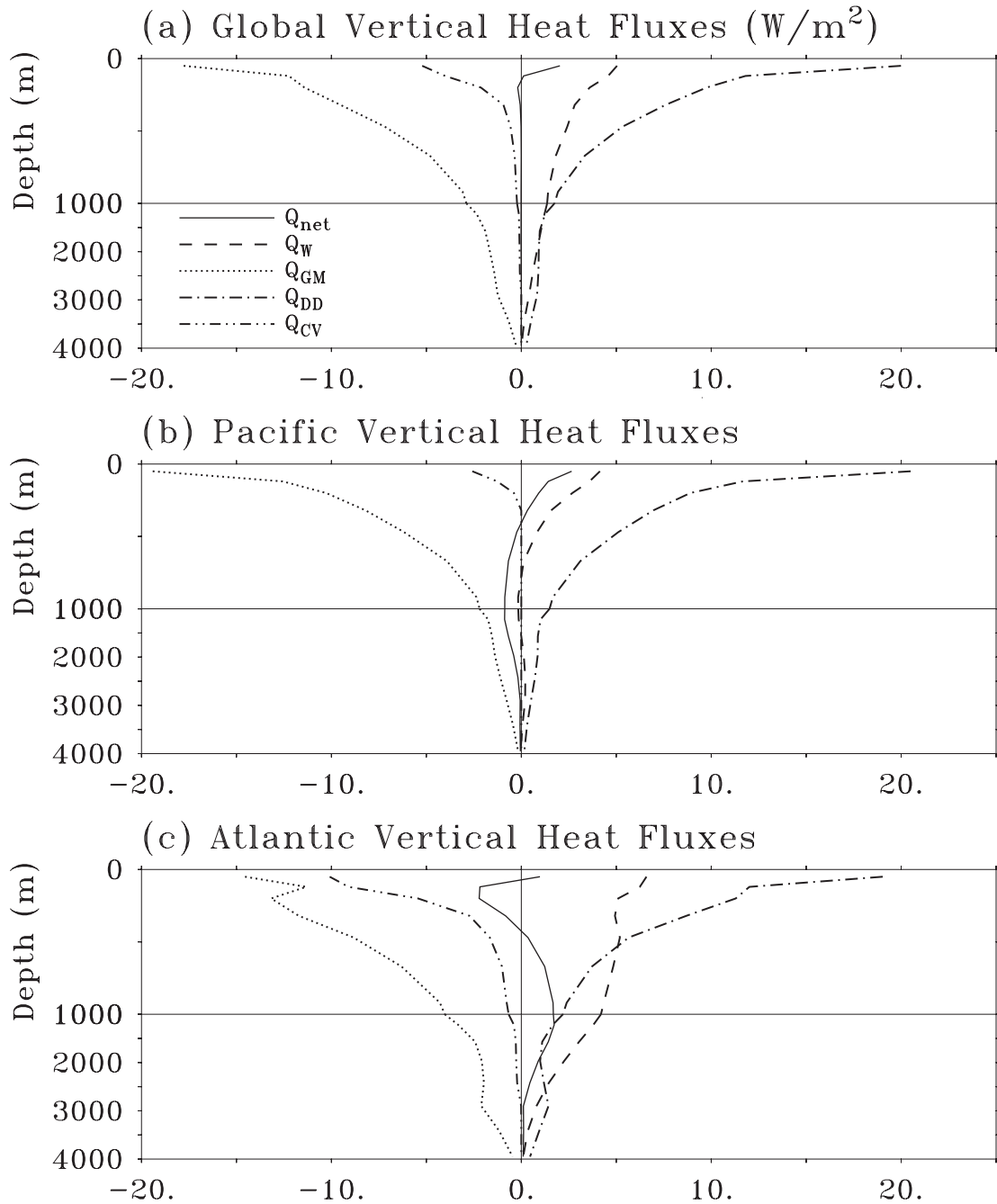


Figure 3. Horizontally integrated vertical heat flux, unit is Wm^{-2} , Positive (negative) values represent downward (upward) flux. (a) Global, (b) Pacific, and (c) Atlantic.

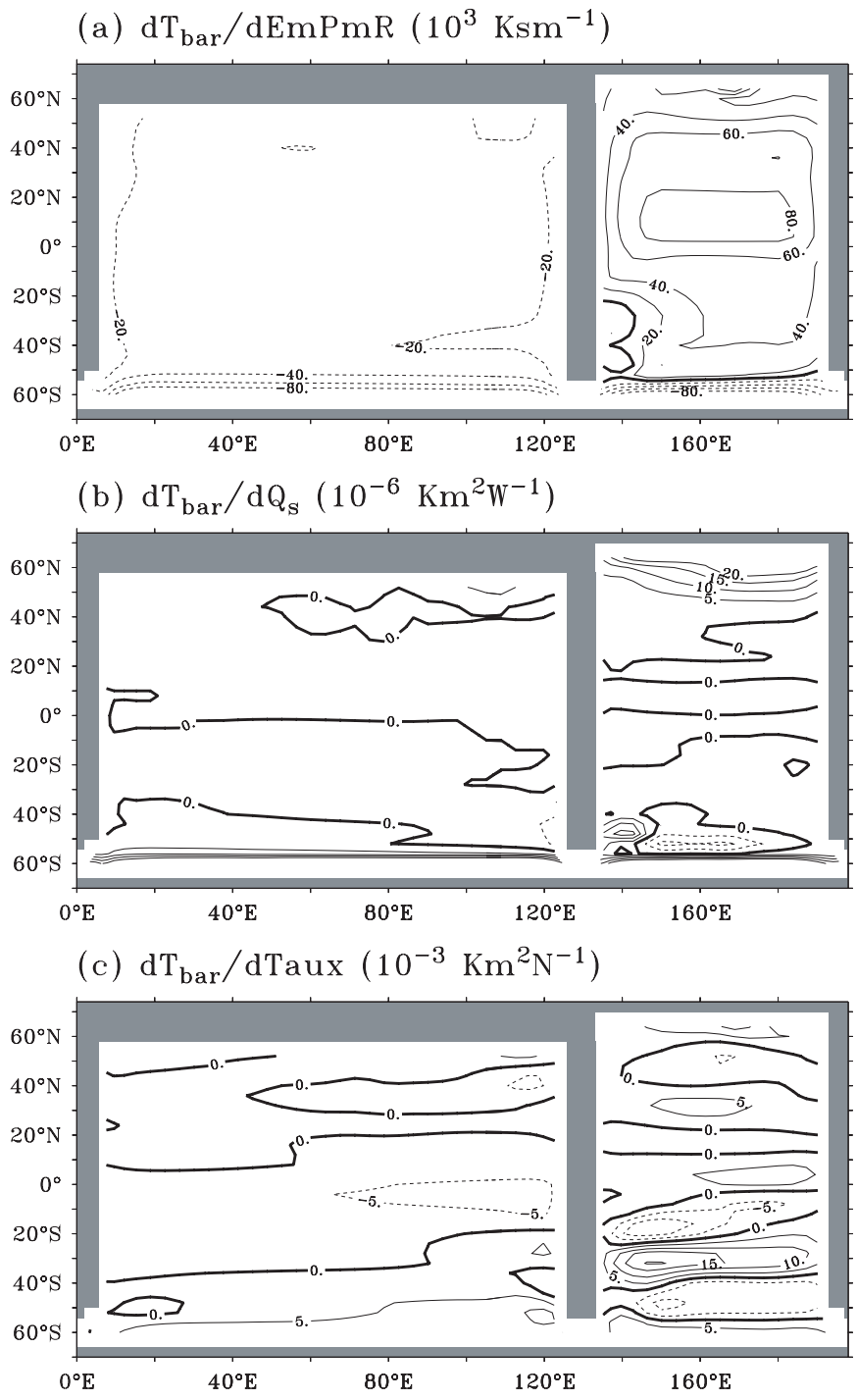


Figure 4. DOC sensitivity at 500 years to (a) Fresh water flux, CI is $20 \times 10^3 \text{ Ksm}^{-1}$, (b) Net surface heat flux, CI is $5 \times 10^{-6} \text{ Km}^2\text{W}^{-1}$, and (c) Zonal wind stress, CI is $5 \times 10^{-3} \text{ Km}^2\text{N}^{-1}$.

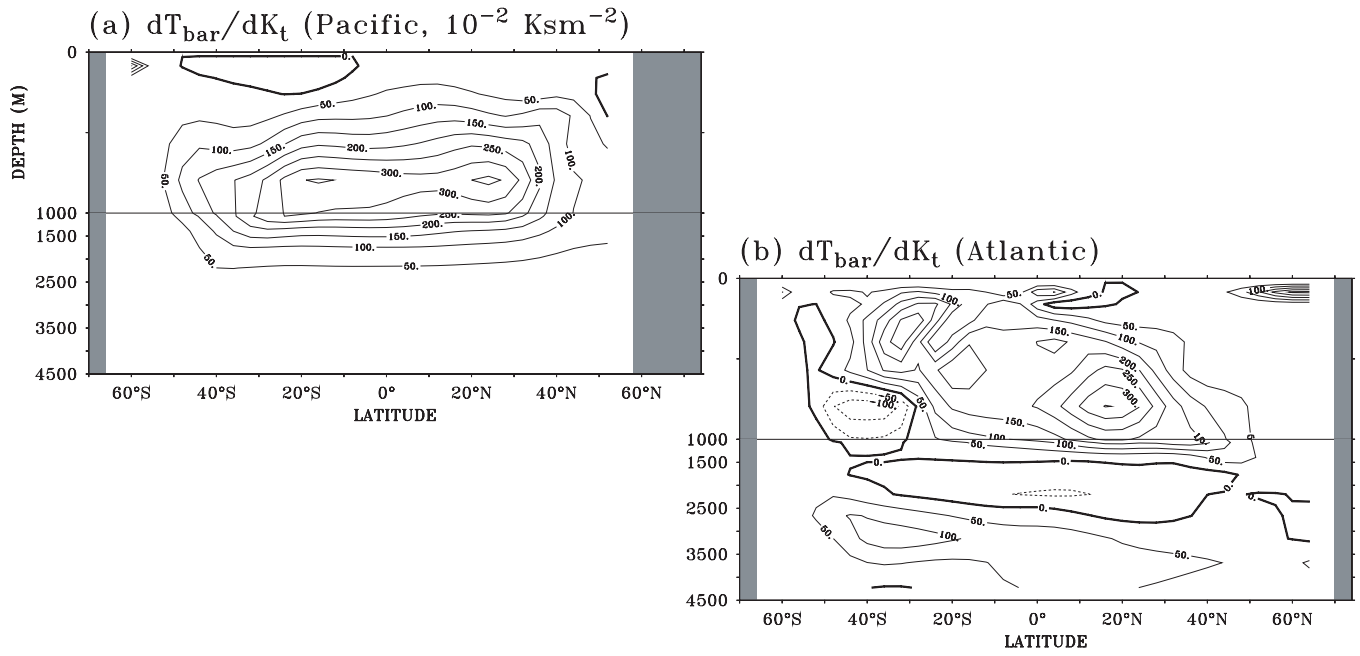


Figure 5. Zonal mean of DOC sensitivity to diapycnal diffusivity of temperature at 500 years, CI is $50 \times 10^{-2} \text{ Ksm}^{-2}$. (a) Pacific, (b) Atlantic.

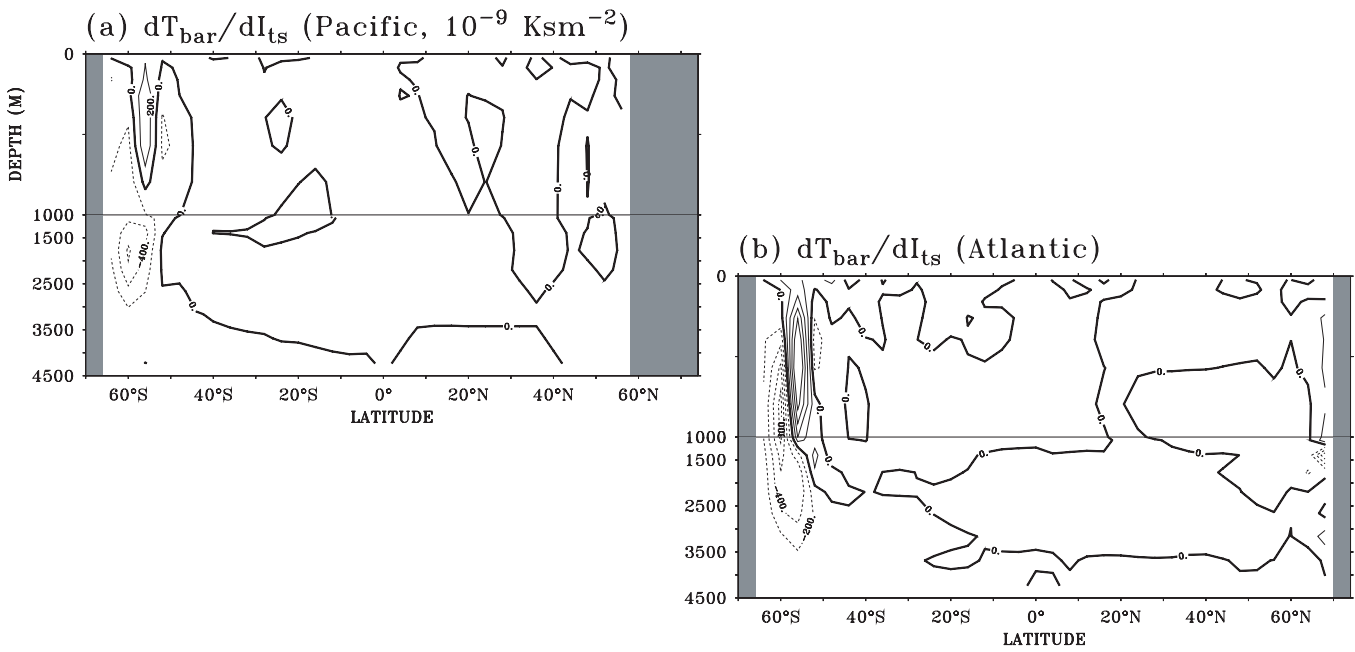


Figure 6. Zonal mean of DOC sensitivity to isopycnal diffusivity for temperature and salinity at 500 years, CI is $100 \times 10^{-9} \text{ Ksm}^{-2}$. (a) Pacific, (b) Atlantic.

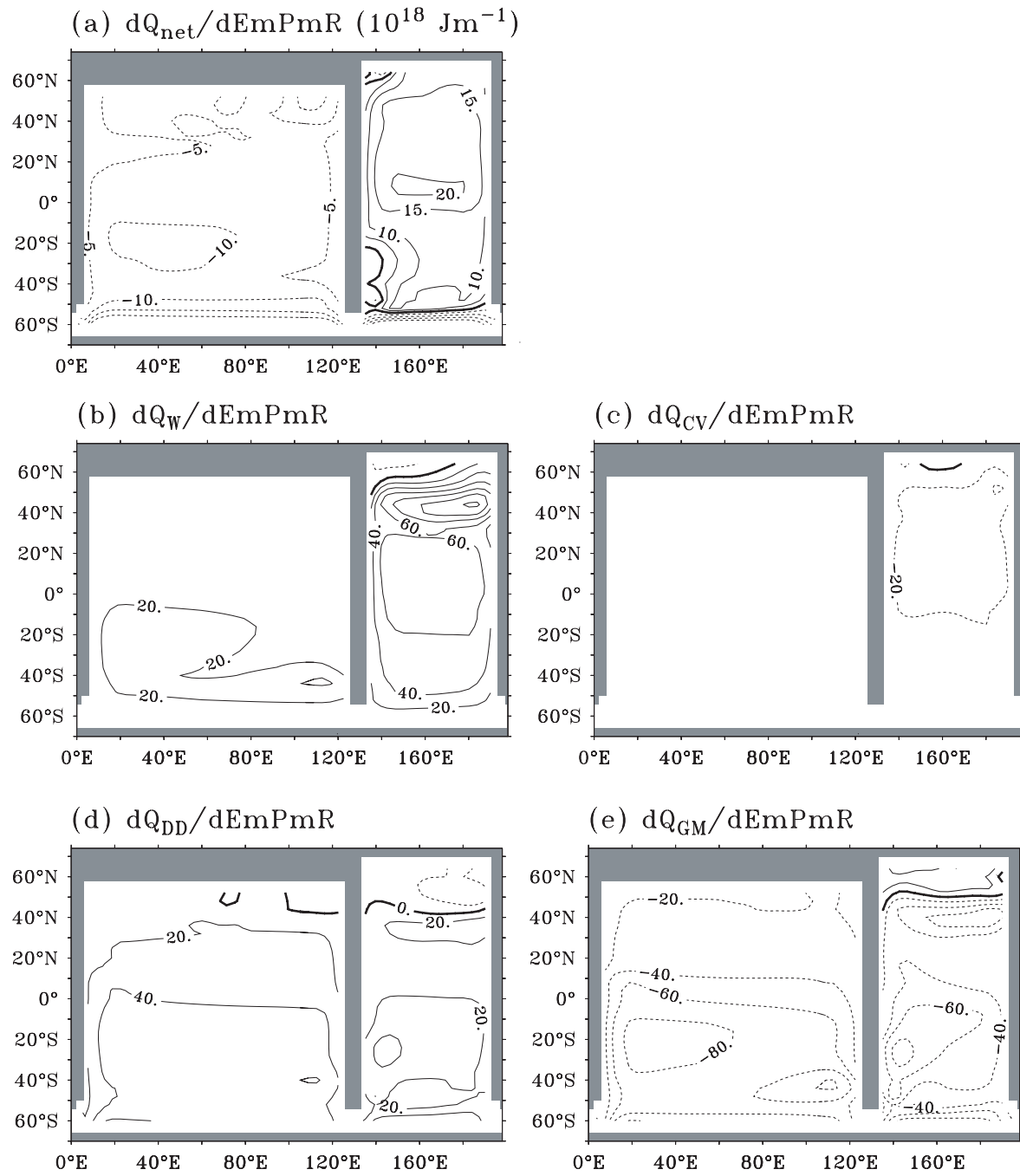


Figure 7. Sensitivities of heat fluxes at 700 m to freshwater flux E-P-R at 100 years. (a) Net heat flux, (b) Vertical advective heat flux, (c) Convective heat flux, (d) Diapycnal diffusive heat flux, and (e) Isopycnal diffusive heat flux. CI is $5 \times 10^{18} \text{ Jm}^{-1}$ in (a), $20 \times 10^{18} \text{ Jm}^{-1}$ from (b) to (e).

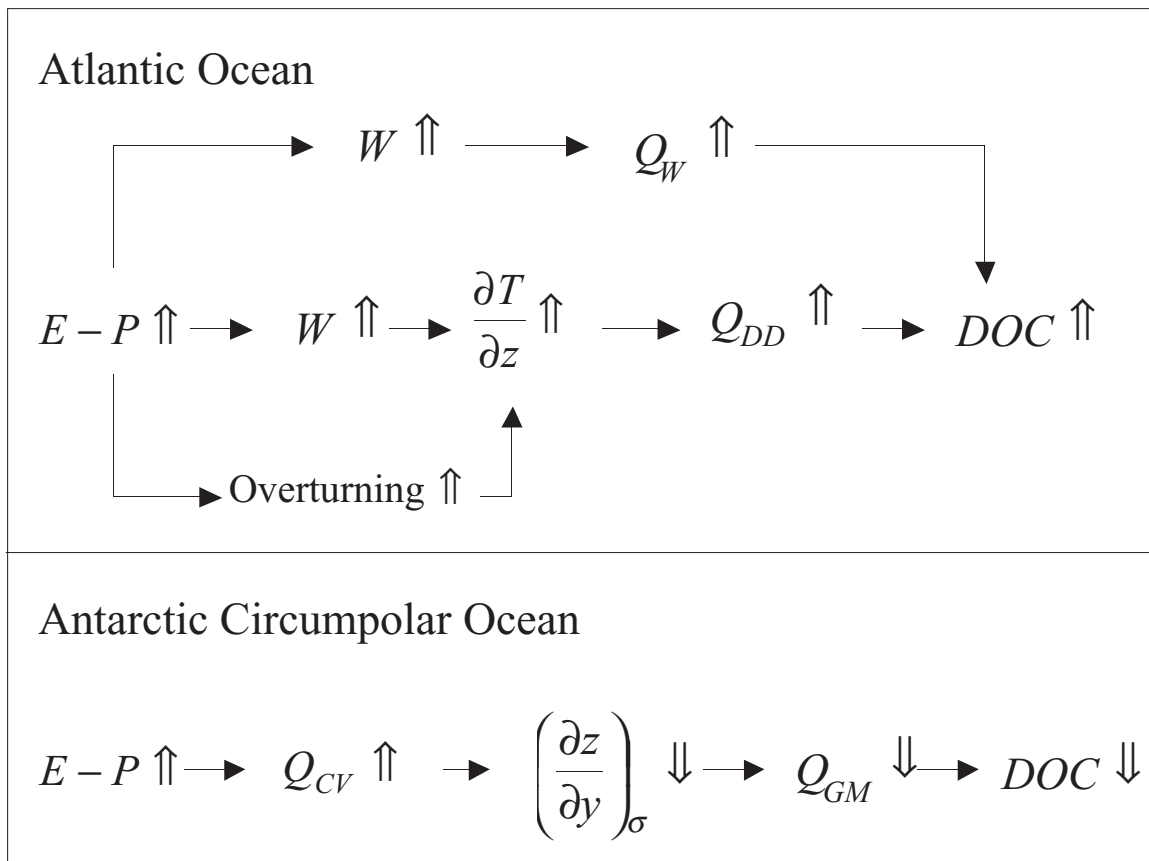


Figure 8. Schematic relationship between E-P-R and DOC. Upward (downward) arrows represent the increase (decrease) of a quantity. All Q's are positive downward.

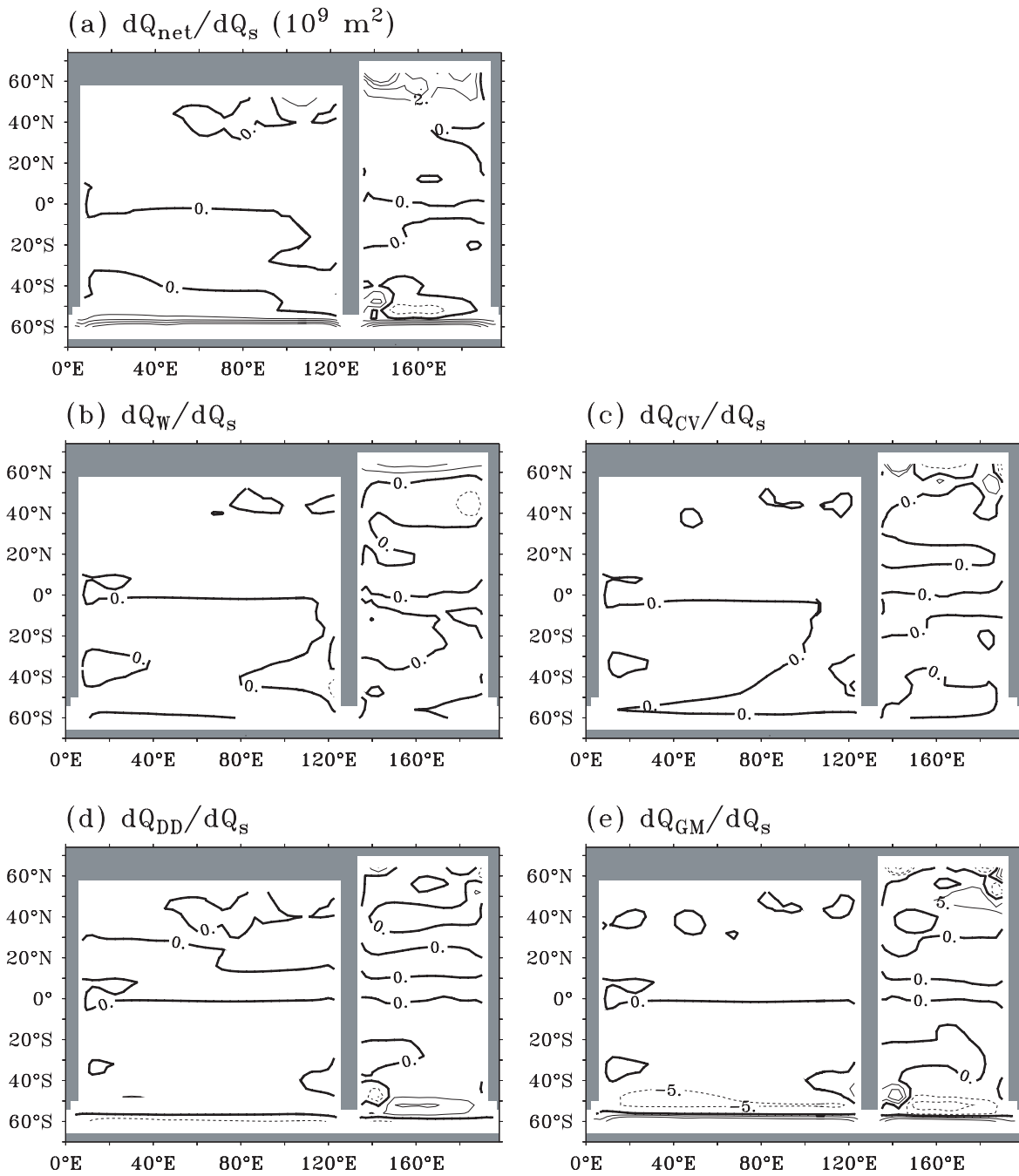


Figure 9. Sensitivities of heat fluxes at 700 m to downward net surface heat flux Q_s at 100 years. (a) Net heat flux, (b) Vertical advective heat flux, (c) Convective heat flux, (d) Diapycnal diffusive heat flux, and (e) Isopycnal diffusive heat flux. CI is $2 \times 10^9 \text{ m}^2$ in (a), $5 \times 10^9 \text{ m}^2$ from (b) to (e).

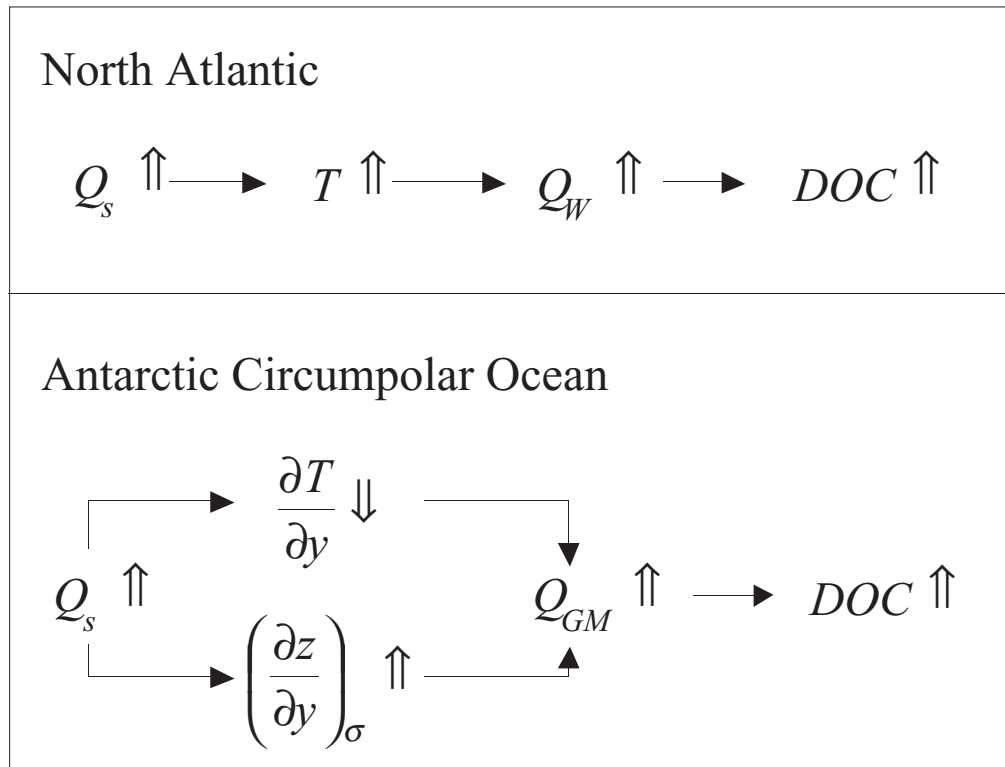


Figure 10. Schematic relationship between downward surface heat flux Q_s and DOC. Upward (downward) arrows represent the increase (decrease) of a quantity. All Q's are positive downward.

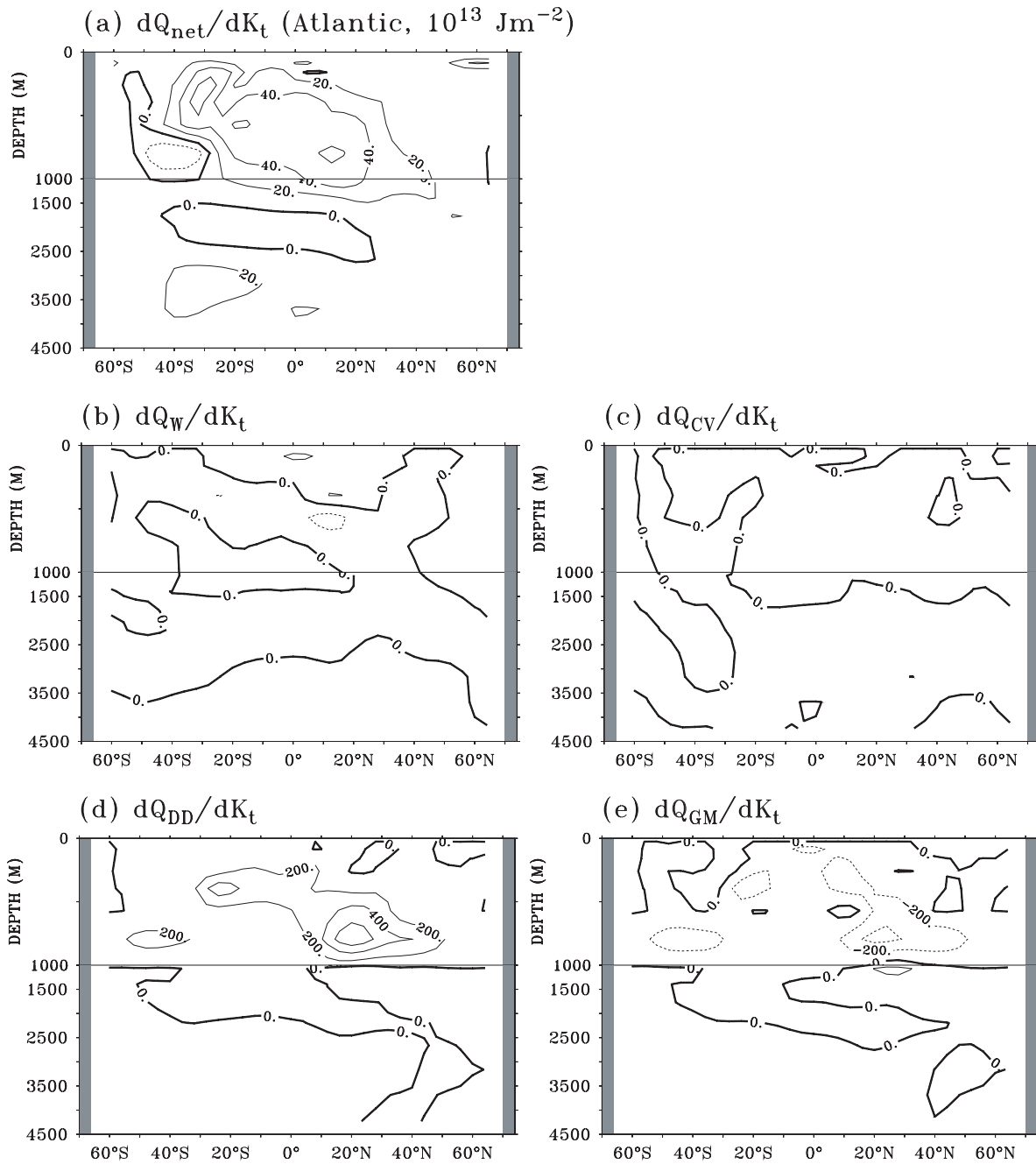


Figure 11. Sensitivities of heat fluxes at 700 m to diapycnal diffusivity of temperature K_t at 100 years in the Atlantic. (a) Net heat flux, (b) Vertical advective heat flux, (c) Convective heat flux, (d) Diapycnal diffusive heat flux, and (e) Isopycnal diffusive heat flux. CI is $20 \times 10^{13} \text{ Jm}^{-2}$ in (a), $200 \times 10^{13} \text{ Jm}^{-2}$ from (b) to (e).

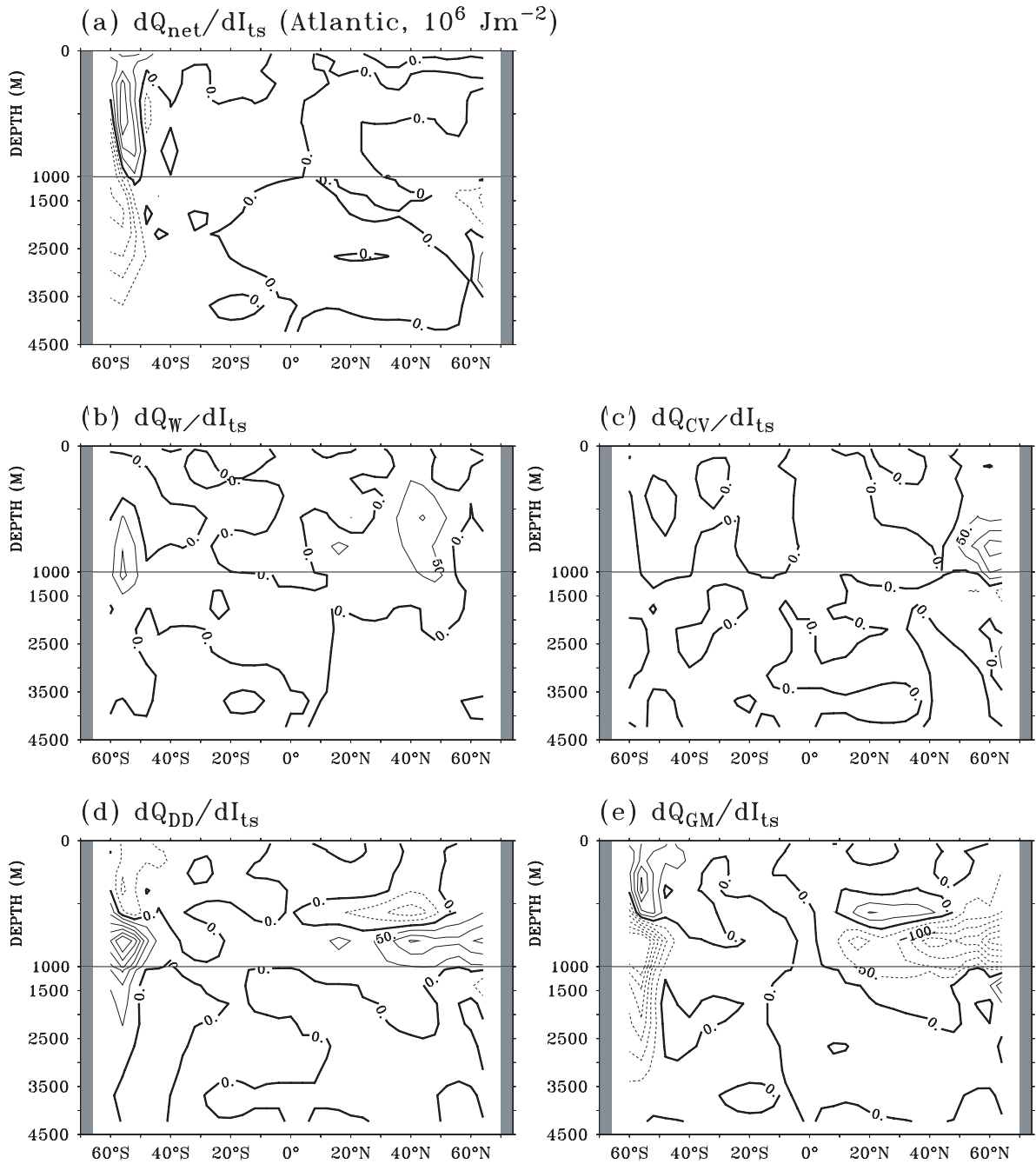


Figure 12. Sensitivities of heat fluxes at 700 m to isopycnal diffusivity for temperature and salinity I_{ts} at 100 years in the Atlantic. (a) Net heat flux, (b) Vertical advective heat flux, (c) Convective heat flux, (d) Diapycnal diffusive heat flux, and (e) Isopycnal diffusive heat flux. CI is $25 \times 10^6 \text{ Jm}^{-2}$ in (a), $50 \times 10^6 \text{ Jm}^{-2}$ from (b) to (e).

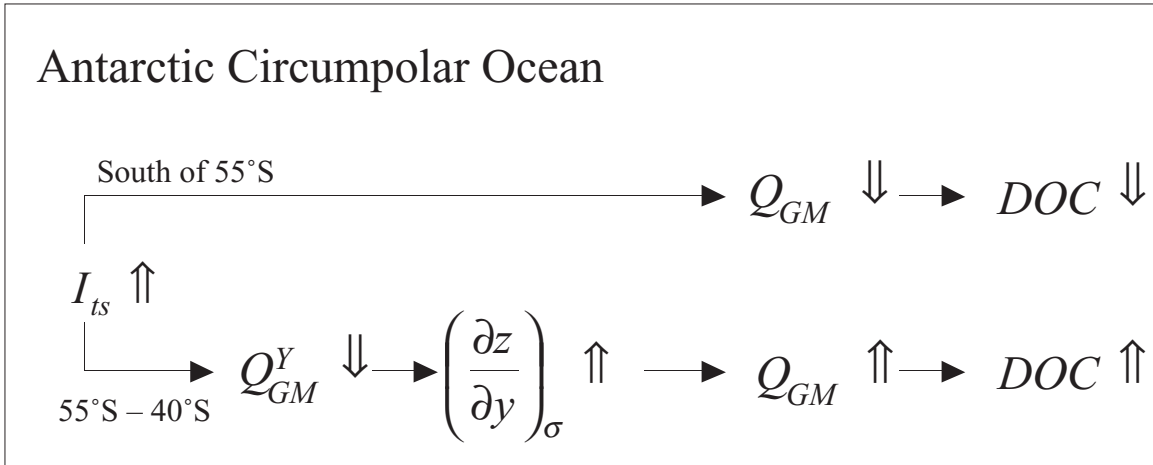


Figure 13. Schematic relationship between isopycnal diffusivity for temperature and salinity I_{ts} and DOC in the South Atlantic. Upward (downward) arrows represent the increase (decrease) of a quantity. All Q's are positive downward.

Table 1. Uncertainties from different parameters. Second column: the uncertainty of DOC below 700 m at the time scale of 500 years, 1°K is equivalent to $3.7 \times 10^{24} J$. Third column: the uncertainty of downward heat flux at 700 m at the time scale of 100 years, Fourth column: the uncertainty of DOC below 700 m at the time scale of 1000 years. Fifth column: the uncertainty of DOC below 200 m at the time scale of 500 years, 1°K is equivalent to $4.2 \times 10^{24} J$.

	$\delta\bar{T}$ (K) 500 yr > 700 m	$\delta\bar{Q}$ (PW) 100 yr > 700 m	$\delta\bar{T}$ (K) 1000 yr > 700 m	$\delta\bar{T}$ (K) 500 yr > 200m
E-P-R	± 0.34	± 0.093	± 0.55	± 0.34
Q_s	± 0.07	± 0.018	± 0.15	± 0.07
τ_x	± 0.14	± 0.053	± 0.20	± 0.17
τ_y	± 0.03	± 0.011	± 0.05	± 0.04
K_r	± 0.40	± 0.127	± 0.55	± 0.47
K_s	± 0.09	± 0.030	± 0.13	± 0.11
I_{ts}	± 0.71	± 0.219	± 1.17	± 0.70

REPORT SERIES of the MIT *Joint Program on the Science and Policy of Global Change*

1. **Uncertainty in Climate Change Policy Analysis** *Jacoby & Prinn* December 1994
2. **Description and Validation of the MIT Version of the GISS 2D Model** *Sokolov & Stone* June 1995
3. **Responses of Primary Production and Carbon Storage to Changes in Climate and Atmospheric CO₂ Concentration** *Xiao et al.* October 1995
4. **Application of the Probabilistic Collocation Method for an Uncertainty Analysis** *Webster et al.* Jan 1996
5. **World Energy Consumption and CO₂ Emissions: 1950-2050** *Schmalensee et al.* April 1996
6. **The MIT Emission Prediction and Policy Analysis (EPPA) Model** *Yang et al.* May 1996
7. **Integrated Global System Model for Climate Policy Analysis** *Prinn et al.* June 1996 (*superseded by No. 36*)
8. **Relative Roles of Changes in CO₂ and Climate to Equilibrium Responses of Net Primary Production and Carbon Storage** *Xiao et al.* June 1996
9. **CO₂ Emissions Limits: *Economic Adjustments and the Distribution of Burdens*** *Jacoby et al.* July 1997
10. **Modeling the Emissions of N₂O & CH₄ from the Terrestrial Biosphere to the Atmosphere** *Liu* Aug 1996
11. **Global Warming Projections: *Sensitivity to Deep Ocean Mixing*** *Sokolov & Stone* September 1996
12. **Net Primary Production of Ecosystems in China and its Equilibrium Responses to Climate Changes** *Xiao et al.* November 1996
13. **Greenhouse Policy Architectures and Institutions** *Schmalensee* November 1996
14. **What Does Stabilizing Greenhouse Gas Concentrations Mean?** *Jacoby et al.* November 1996
15. **Economic Assessment of CO₂ Capture and Disposal** *Eckaus et al.* December 1996
16. **What Drives Deforestation in the Brazilian Amazon?** *Pfaff* December 1996
17. **A Flexible Climate Model For Use In Integrated Assessments** *Sokolov & Stone* March 1997
18. **Transient Climate Change & Potential Croplands of the World in the 21st Century** *Xiao et al.* May 1997
19. **Joint Implementation: *Lessons from Title IV's Voluntary Compliance Programs*** *Atkeson* June 1997
20. **Parameterization of Urban Sub-grid Scale Processes in Global Atmospheric Chemistry Models** *Calbo et al.* July 1997
21. **Needed: A Realistic Strategy for Global Warming** *Jacoby, Prinn & Schmalensee* August 1997
22. **Same Science, Differing Policies; *The Saga of Global Climate Change*** *Skolnikoff* August 1997
23. **Uncertainty in the Oceanic Heat & Carbon Uptake & their Impact on Climate Projections** *Sokolov et al.* Sep 1997
24. **A Global Interactive Chemistry and Climate Model** *Wang, Prinn & Sokolov* September 1997
25. **Interactions Among Emissions, Atmospheric Chemistry and Climate Change** *Wang & Prinn* Sep 1997
26. **Necessary Conditions for Stabilization Agreements** *Yang & Jacoby* October 1997
27. **Annex I Differentiation Proposals: *Implications for Welfare, Equity and Policy*** *Reiner & Jacoby* Oct 1997
28. **Transient Climate Change & Net Ecosystem Production of the Terrestrial Biosphere** *Xiao et al.* Nov 1997
29. **Analysis of CO₂ Emissions from Fossil Fuel in Korea: 1961–1994** *Choi* November 1997
30. **Uncertainty in Future Carbon Emissions: *A Preliminary Exploration*** *Webster* November 1997
31. **Beyond Emissions Paths: *Rethinking the Climate Impacts of Emissions Protocols*** *Webster & Reiner* Nov 1997
32. **Kyoto's Unfinished Business** *Jacoby, Prinn & Schmalensee* June 1998
33. **Economic Development and the Structure of the Demand for Commercial Energy** *Judson et al.* April 1998
34. **Combined Effects of Anthropogenic Emissions and Resultant Climatic Changes on Atmospheric OH** *Wang & Prinn* April 1998
35. **Impact of Emissions, Chemistry, and Climate on Atmospheric Carbon Monoxide** *Wang & Prinn* Apr 1998
36. **Integrated Global System Model for Climate Policy Assessment: *Feedbacks and Sensitivity Studies*** *Prinn et al.* June 1998
37. **Quantifying the Uncertainty in Climate Predictions** *Webster & Sokolov* July 1998
38. **Sequential Climate Decisions Under Uncertainty: *An Integrated Framework*** *Valverde et al.* Sep 1998
39. **Uncertainty in Atm. CO₂ (Ocean Carbon Cycle Model Analysis)** *Holian* Oct 1998 (*superseded by No. 80*)
40. **Analysis of Post-Kyoto CO₂ Emissions Trading Using Marginal Abatement Curves** *Ellerman & Decaux* Oct 1998
41. **The Effects on Developing Countries of the Kyoto Protocol & CO₂ Emissions Trading** *Ellerman et al.* Nov 1998
42. **Obstacles to Global CO₂ Trading: *A Familiar Problem*** *Ellerman* November 1998
43. **The Uses and Misuses of Technology Development as a Component of Climate Policy** *Jacoby* Nov 1998
44. **Primary Aluminum Production: *Climate Policy, Emissions and Costs*** *Harnisch et al.* December 1998
45. **Multi-Gas Assessment of the Kyoto Protocol** *Reilly et al.* January 1999
46. **From Science to Policy: *The Science-Related Politics of Climate Change Policy in the U.S.*** *Skolnikoff* Jan 1999

Contact the Joint Program Office to request a copy. The Report Series is distributed at no charge.

REPORT SERIES of the MIT *Joint Program on the Science and Policy of Global Change*

47. **Constraining Uncertainties in Climate Models Using Climate Change Detection Techniques** *Forest et al.* April 1999
48. **Adjusting to Policy Expectations in Climate Change Modeling** *Shackley et al.* May 1999
49. **Toward a Useful Architecture for Climate Change Negotiations** *Jacoby et al.* May 1999
50. **A Study of the Effects of Natural Fertility, Weather and Productive Inputs in Chinese Agriculture** *Eckaus & Tso* July 1999
51. **Japanese Nuclear Power and the Kyoto Agreement** *Babiker, Reilly & Ellerman* August 1999
52. **Interactive Chemistry and Climate Models in Global Change Studies** *Wang & Prinn* September 1999
53. **Developing Country Effects of Kyoto-Type Emissions Restrictions** *Babiker & Jacoby* October 1999
54. **Model Estimates of the Mass Balance of the Greenland and Antarctic Ice Sheets** *Bugnion* Oct 1999
55. **Changes in Sea-Level Associated with Modifications of the Ice Sheets over the 21st Century** *Bugnion* October 1999
56. **The Kyoto Protocol and Developing Countries** *Babiker, Reilly & Jacoby* October 1999
57. **A Game of Climate Chicken: Can EPA regulate GHGs before the Senate ratifies the Kyoto Protocol?** *Bugnion & Reiner* Nov 1999
58. **Multiple Gas Control Under the Kyoto Agreement** *Reilly, Mayer & Harnisch* March 2000
59. **Supplementarity: An Invitation for Monopsony?** *Ellerman & Sue Wing* April 2000
60. **A Coupled Atmosphere-Ocean Model of Intermediate Complexity** *Kamenkovich et al.* May 2000
61. **Effects of Differentiating Climate Policy by Sector: A U.S. Example** *Babiker et al.* May 2000
62. **Constraining climate model properties using optimal fingerprint detection methods** *Forest et al.* May 2000
63. **Linking Local Air Pollution to Global Chemistry and Climate** *Mayer et al.* June 2000
64. **The Effects of Changing Consumption Patterns on the Costs of Emission Restrictions** *Lahiri et al.* Aug 2000
65. **Rethinking the Kyoto Emissions Targets** *Babiker & Eckaus* August 2000
66. **Fair Trade and Harmonization of Climate Change Policies in Europe** *Viguié* September 2000
67. **The Curious Role of "Learning" in Climate Policy: Should We Wait for More Data?** *Webster* October 2000
68. **How to Think About Human Influence on Climate** *Forest, Stone & Jacoby* October 2000
69. **Tradable Permits for Greenhouse Gas Emissions: A primer with particular reference to Europe** *Ellerman* November 2000
70. **Carbon Emissions and The Kyoto Commitment in the European Union** *Viguié et al.* February 2001
71. **The MIT Emissions Prediction and Policy Analysis (EPPA) Model: Revisions, Sensitivities, and Comparisons of Results** *Babiker et al.* February 2001
72. **Cap and Trade Policies in the Presence of Monopoly & Distortionary Taxation** *Fullerton & Metcalf* Mar 2001
73. **Uncertainty Analysis of Global Climate Change Projections** *Webster et al.* March 2001
74. **The Welfare Costs of Hybrid Carbon Policies in the European Union** *Babiker et al.* June 2001
75. **Feedbacks Affecting the Response of the Thermohaline Circulation to Increasing CO₂** *Kamenkovich et al.* July 2001
76. **CO₂ Abatement by Multi-fueled Electric Utilities: An Analysis Based on Japanese Data** *Ellerman & Tsukada* July 2001
77. **Comparing Greenhouse Gases** *Reilly, Babiker & Mayer* July 2001
78. **Quantifying Uncertainties in Climate System Properties using Recent Climate Observations** *Forest et al.* July 2001
79. **Uncertainty in Emissions Projections for Climate Models** *Webster et al.* August 2001
80. **Uncertainty in Atmospheric CO₂ Predictions from a Parametric Uncertainty Analysis of a Global Ocean Carbon Cycle Model** *Holian, Sokolov & Prinn* September 2001
81. **A Comparison of the Behavior of Different AOGCMs in Transient Climate Change Experiments** *Sokolov, Forest & Stone* December 2001
82. **The Evolution of a Climate Regime: Kyoto to Marrakech** *Babiker, Jacoby & Reiner* February 2002
83. **The "Safety Valve" and Climate Policy** *Jacoby & Ellerman* February 2002
84. **A Modeling Study on the Climate Impacts of Black Carbon Aerosols** *Wang* March 2002
85. **Tax Distortions and Global Climate Policy** *Babiker, Metcalf & Reilly* May 2002
86. **Incentive-based Approaches for Mitigating GHG Emissions: Issues and Prospects for India** *Gupta* June 2002
87. **Sensitivities of Deep-Ocean Heat Uptake and Heat Content to Surface Fluxes and Subgrid-Scale Parameters in an Ocean GCM with Idealized Geometry** *Huang, Stone & Hill* September 2002
88. **The Deep-Ocean Heat Uptake in Transient Climate Change** *Huang et al.* September 2002